IMMUNOLOGY

T cell–derived soluble glycoprotein GPIbα mediates PGE_2 production in human monocytes activated with the vaccine adjuvant MDP

Fengjie Liu[1]*, Yukinori Endo[1]*†, Tatiana Romantseva[1], Wells W. Wu[2], Adovi Akue[3], Rong-Fong Shen[2], Hana Golding[1], Marina Zaitseva[1]‡

Vaccine adjuvants containing analogs of microbial products activate pattern recognition receptors (PRRs) on antigen-presenting cells, including monocytes and macrophages, which can cause prostaglandin E_2 (PGE_2) release and consequently undesired inflammatory responses and fever in vaccine recipients. Here, we studied the mechanism of PGE_2 production by human monocytes activated with muramyl dipeptide (MDP) adjuvant, which activates cytosolic nucleotide-binding oligomerization domain 2 (NOD2). In rabbits, administration of MDP elicited an early increase in PGE_2 followed by fever. In human monocytes, MDP alone did not induce PGE_2 production. However, high amounts of PGE_2 and the proinflammatory cytokines IL-1β and IL-6 were secreted by monocytes activated with MDP in the presence of conditioned medium obtained from CD3 bead–isolated T cells (Tc CM) but not from those isolated without CD3 beads. Mass spectrometry and immunoblotting revealed that the costimulatory factor in Tc CM was glycoprotein Ib α (GPIbα). Antibody-mediated blockade of GPIbα or of its receptor, Mac-1 integrin, inhibited the secretion of PGE_2, IL-1β, and IL-6 in MDP + Tc CM–activated monocytes, whereas recombinant GPIbα protein increased PGE_2 production by MDP-treated monocytes. In vivo, *COX2* mRNA abundance was reduced in the liver and spleen of Mac-1 KO mice after administration of MDP compared with that of treated wild-type mice. Our findings suggest that the production of PGE_2 and proinflammatory cytokines by MDP-activated monocytes is mediated by cooperation between two signaling pathways: one delivered by MDP through NOD2 and a second through activation of Mac-1 by T cell–derived GPIbα.

INTRODUCTION

Adjuvants are added to vaccine formulations to augment immune responses to the vaccine antigens by enhancing antigen processing and presentation by antigen-presenting cells (APCs). Many adjuvants are composed of naturally derived microbial products or their synthetic analogs. Adjuvants interact with a battery of pattern recognition receptors (PRRs) expressed on APCs such as dendritic cells and macrophages. In some cases, excessive activation of PRRs on APCs may lead to local and systemic toxicities, including fever. Of the total number of reported cases submitted to the Vaccine Adverse Event Reporting System in 1991 to 2001, fever was the most commonly observed adverse event that appeared in 25.8% reports, followed by injection site hypersensitivity (15.8%), rash (11.0%), injection site edema (10.8%), and vasodilatation (10.8%) (*1*).

Macrophages produce pyrogenic cytokines such as interleukin-1β (IL-1β), IL-6, and tumor necrosis factor–α upon activation of PRRs by microbial products. Pyrogenic cytokines released by macrophages are transported via the blood stream to the ventromedial preoptic area in the hypothalamus, where they induce release of a thermogenic lipid mediator prostaglandin E_2 (PGE_2) (*2*). In addition to central production in the brain, PGE_2 can be produced in peripheral tissues by macrophages, including Kupffer cells in the liver (*3*, *4*). It has been shown that locally produced PGE_2 can transmit a febrile signal by binding to PGE_2 receptors expressed either on peripheral sensory neurons present in many organs—including kidneys, lungs, and stomach (*5*–*7*)—or upon transport to the brain as an albumin-bound complex (*8*, *9*).

Muramyl dipeptide (MDP) is a peptidoglycan motif present in all Gram-positive and Gram-negative bacteria. MDP can serve as a minimal structure and replace the activity of the whole killed mycobacterium in complete Freund's adjuvant (CFA) (*10*). Studies in animals established that MDP exerts a broad array of immune-modulating activities including enhancement of antibody production, increased cell-mediated immunity, increased nonspecific immunity to bacteria, and increased cytokine release (*11*). MDP is recognized by the cytosolic PRR NOD2 (nucleotide-binding oligomerization domain 2) (*12*, *13*). NOD2 is highly expressed in APCs and is required for a humoral response to antigens adjuvanted with MDP (*14*, *15*). Because CFA is toxic for human use, efforts have been made to develop safer adjuvants based on MDP (*16*). MDP-derived murabutide, threonyl-MDP, and muramyl tripeptide were tested in clinical trials as part of vaccines against HIV-1 and influenza viruses (*17*, *18*). Substantial reactogenicity, including fever and other systemic reactions, was observed in a proportion of vaccines and blunted further development of MDP adjuvant for human vaccines (*19*, *20*). Although the ability of MDP to induce fever has been well established, the underlying mechanisms, including PGE_2 induction in primary cells by MDP, have not been fully elucidated.

Here, we used MDP as a prototype adjuvant with pyrogenic potential to investigate the mechanism of PGE_2 production. Our data showed that MDP-induced PGE_2 production in human primary

[1]Division of Viral Products, Food and Drug Administration, Silver Spring, MD 20993, USA. [2]Facility for Biotechnology Resources, Food and Drug Administration, Silver Spring, MD 20993, USA. [3]Flow Cytometry Core, Center for Biologics Evaluation and Research (CBER), Food and Drug Administration, Silver Spring, MD 20993, USA.
*These authors contributed equally to this work.
†Present address: Division of Biotechnology Research and Review I, Center for Drug Evaluation and Research (CDER), Food and Drug Administration, Silver Spring, MD 20993, USA.
‡Corresponding author. Email: marina.zaitseva@fda.hhs.gov

monocytes was strongly increased in the presence of glycoprotein Ib α (GPIbα) protein derived from T cells, suggesting that a cross-talk between adjuvant-triggered PRRs and T cell–triggered macrophage-1 antigen (Mac-1) integrin may play a critical role in production of proinflammatory mediators by monocytes.

RESULTS

MDP induces pyrogenic response in New Zealand white rabbits

Early clinical trials of MDP-adjuvanted HIV-1 and influenza vaccines showed systemic toxicity in subjects including fever (*17*, *19*, *20*). To determine the mechanism of the MDP-induced pyrogenic response, New Zealand white (NZW) rabbits were administered MDP at 10 or 30 μg/kg or phosphate-buffered saline (PBS) in control. Body temperatures were recorded, and blood samples were collected in rabbits before treatment (time 0) and up to 72 hours after treatment (Fig. 1). No increases in body temperature were detected in PBS-treated animals. Rabbits that received MDP at 10 and 30 μg/kg showed elevation in body temperature reaching an increase of 0.6° to 1.2°C and 1.4° to 1.7°C, respectively, at 5 hours after treatment compared with time 0 (Fig. 1A). Body temperature returned to baseline levels in all MDP-inoculated rabbits by 24 hours. C-reactive protein (CRP) in the blood of MDP-injected rabbits increased about 8.0- to 16.0-fold at 24 hours after treatment and returned to baseline levels by 72 hours (Fig. 1B). These finding showed that inoculation of MDP in rabbits induced a rapid pyrogenic response.

Previously, we have shown that increase in plasma PGE_2 preceded the rise in body temperature in rabbits inoculated with the Toll-like receptor (TLR) agonists mycoplasmal lipopeptide FSL-1 or flagellin (*21*). In the current study, PGE_2 increased in all six rabbits inoculated with MDP at 1 hour after treatment in a dose-dependent manner and returned to background levels at 3 hours after treatment (Fig. 1C). PGE_2 did not increase in rabbits inoculated with PBS. These data suggest a role for early PGE_2 production in the observed increase in body temperature in rabbits inoculated with MDP (Fig. 1C).

Human T cells stimulate monocytes to produce PGE_2 in response to MDP in vitro

To determine whether MDP induces PGE_2 production in human peripheral blood mononuclear cells (PBMCs), MDP was added to cultures of human PBMC or monocyte-depleted PBMCs (PBMC-Mo) or to monocytes alone (Fig. 2A). Very low levels of PGE_2 were measured in untreated PBMCs or in PBMC-Mo. MDP induced high levels of PGE_2 in PBMCs but not in PBMC-Mo, suggesting that monocytes are the main source of PGE_2 in PBMCs (Fig. 2A). Unexpectedly, MDP-treated monocytes produced minimal amount of PGE_2 compared with PBMCs (Fig. 2A). In search for other cell types that might provide help to monocytes, T cells were purified from PBMCs using CD3 microbeads and were added to monocytes (Mo + Tc). MDP-treated monocytes produced high levels of PGE_2 when cocultured with T cells compared with treatment of monocytes with MDP alone (Fig. 2A).

A soluble factor produced by T cells induces PGE_2 and proinflammatory cytokines in MDP-activated monocytes

To determine whether cell-to-cell contact between T cells and monocytes is required for PGE_2 production, monocytes were treated with MDP alone (500 ng/ml) or were cocultured with CD3 bead–purified T cells in separate chambers of a transwell plate (MDP/Tc) (Fig. 2B). Monocytes treated with MDP produced 15-fold higher levels of PGE_2 when cocultured with T cells in transwell plate compared with MDP treatment alone (Fig. 2B). Conditioned medium (CM) from CD3 bead–purified T cells cultured overnight in the absence of MDP (Tc CM) induced high levels of PGE_2 when added to monocytes in combination with MDP (MDP/Tc CM); no PGE_2 was induced by Tc CM (Fig. 2B). A further increase in the dose of MDP to 2500 ng/ml did not result in high levels of PGE_2 production in the absence of Tc CM, suggesting that even high dose of MDP was insufficient to activate monocytes (fig. S1).

To determine whether treatment with CD3 microbeads followed by overnight incubation triggers PGE_2-inducing activity in T cells, CM was prepared from T cells purified using CD3 beads (positive selection) or from T cells purified by negative selection (NS T cells). Tc CM prepared from 22 donors of PBMCs induced 6- to 30-fold increase in PGE_2 in MDP-treated monocytes; at the same time, no increase in PGE_2 production was measured in MDP-treated monocytes supplemented with CM from the NS T cells (NSTc CM) from the same individuals (table S1). CM from NS T cells that were incubated with CD3 microbeads increased PGE_2 production in MDP-treated monocytes compared with MDP alone, suggesting that low-level activation induced T cell–derived factor that augments PGE_2 production in MDP-treated monocytes (fig. S2).

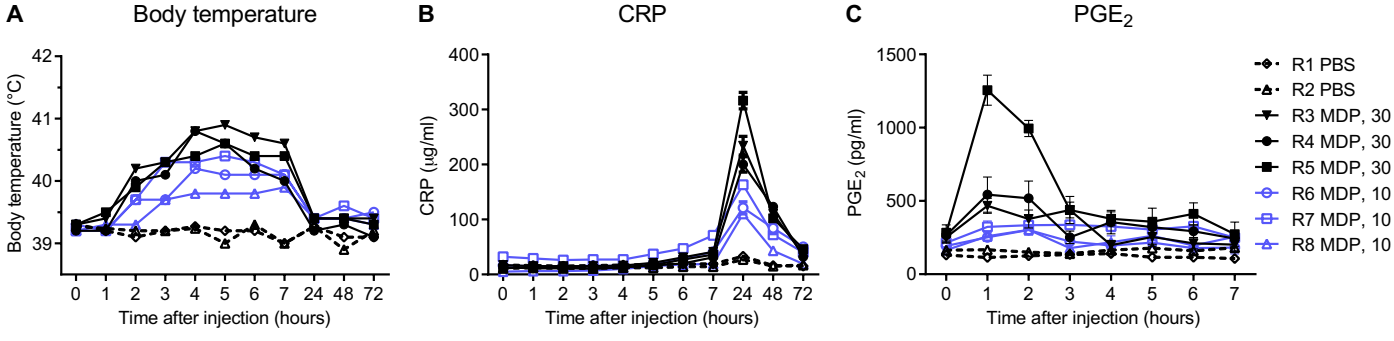

Fig. 1. Administration of MDP in rabbits induced fever and increased CRP and PGE_2 in the blood. (**A** to **C**) Female NZW rabbits ($n = 8$) were inoculated with PBS (R1 and R2) or with MDP at 30 or 10 μg/kg (R3, R4, and R5 and R6, R7, and R8, respectively) at time 0. Body temperatures were recorded (A), and CRP (B) and PGE_2 (C) were measured in blood samples at time 0 and up to either 72 hours (A and B) or 7 hours (C) after treatment. Data are shown as body temperature measured in each rabbit at indicated time points (A) or as means ± SD calculated for triplicate wells (B and C).

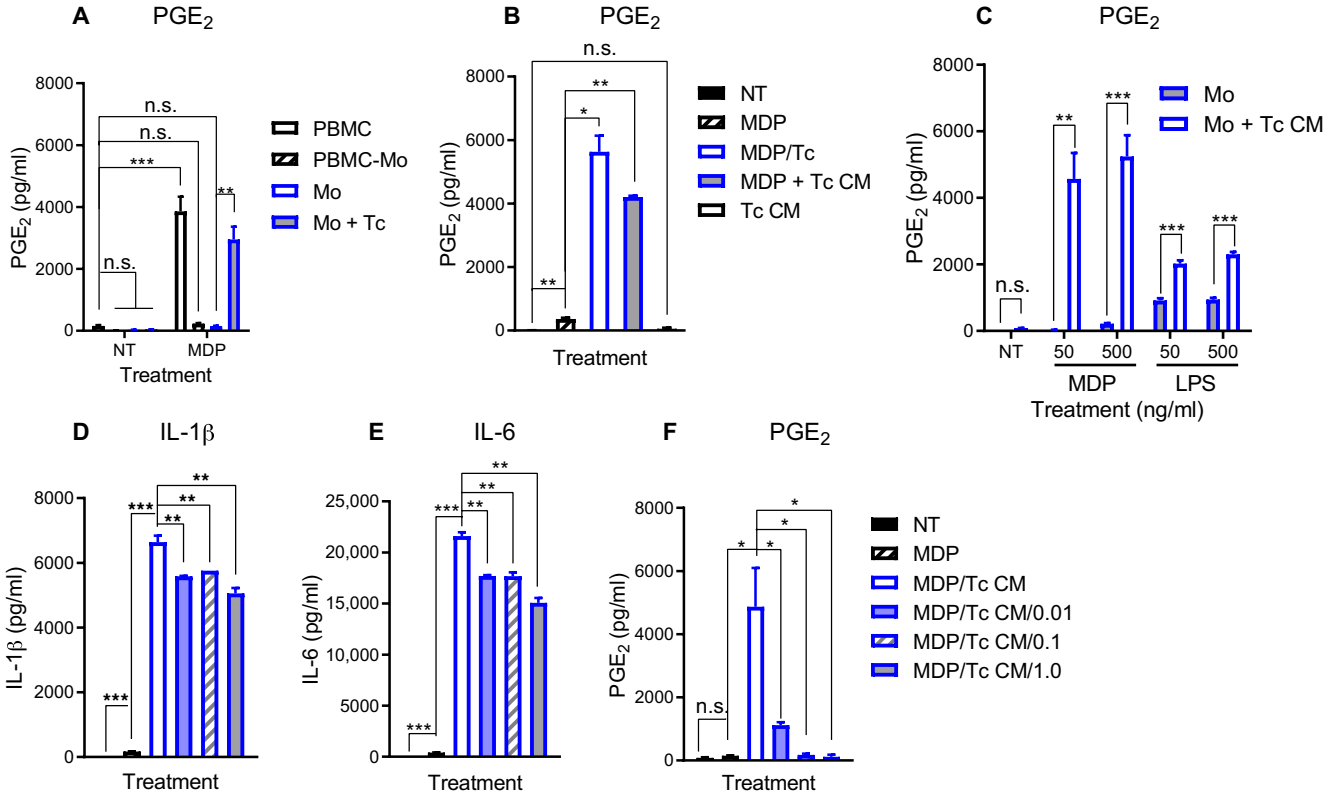

Fig. 2. Soluble factor produced by T cells augmented production of PGE_2 and proinflammatory cytokines in human monocytes activated with MDP. (**A**) Quantification of PGE_2 in cultures of PBMC, monocyte-depleted PBMC (PBMC-Mo), monocytes alone (Mo), and monocytes cocultured with CD3 bead–purified T cells (Mo + Tc) and either not treated (NT) or incubated with MDP overnight. $^{**}P \leq 0.01$; $^{***}P \leq 0.001$; and n.s., not significant ($P > 0.05$), by two-tailed unpaired *t* test. (**B**) Quantification of PGE_2 in cultures of monocytes not treated (NT) or treated with MDP alone (MDP), with MDP and CD3 bead–purified T cells in separate chambers of transwell plate (MDP/Tc), with MDP and Tc CM (MDP + Tc CM), or with Tc CM alone overnight. $^{*}P \leq 0.05$; $^{**}P \leq 0.01$; and n.s., not significant ($P > 0.05$), by two-tailed unpaired *t* test. (**C**) Quantification of PGE_2 in monocytes incubated alone (Mo) or incubated with Tc CM (Mo + Tc CM) overnight not treated (NT) or treated with MDP or LPS at 50 or 500 ng/ml.$^{**}P \leq 0.01$; $^{***}P \leq 0.001$; and n.s., not significant ($P > 0.05$), by two-tailed unpaired *t* test. (**D** to **F**) Quantification of IL-1β (D), IL-6 (E), and PGE_2 (F) in monocytes incubated with MDP or with MDP and Tc CM alone (MDP/Tc CM) or in the presence of 0.01, 0.1, or 1.0 μM indomethacin. Data are means ± SD calculated for triplicate wells in a representative of three experiments performed with cells from individual donors. $^{*}P \leq 0.05$; $^{**}P \leq 0.01$; $^{***}P \leq 0.001$; and n.s., not significant ($P > 0.05$), by two-tailed unpaired *t* test.

To determine whether Tc CM also amplifies production of PGE_2 in monocytes activated with lipopolysaccharide (LPS), monocytes were cultured overnight with MDP or with LPS at 50 or 500 ng/ml alone or in the presence of Tc CM (Fig. 2C). Tc CM induced a 200- and 24-fold increase in PGE_2 production in monocytes treated with MDP at 50 and 500 ng/ml, compared with MDP alone, respectively, whereas only 2-fold increase in PGE_2 was induced by Tc CM in LPS-treated monocytes (Fig. 2C). These data suggest that Tc CM plays a critical role in PGE_2 production in monocytes activated with MDP compared with LPS.

In addition to PGE_2, cell culture supernatants from monocytes were assayed for IL-1β and IL-6 proinflammatory cytokines. Tc CM induced about 40- to 50-fold increase in production of IL-1β and of IL-6 in MDP-treated monocytes compared with MDP treatment alone (Fig. 2, D and E). A COX-2 inhibitor, indomethacin, added to monocytes (0.01 to 1.0 μM) reduced production of PGE_2 by 77 to 98% (Fig. 2F). In contrast, IL-1β and of IL-6 cytokines were only modestly reduced by indomethacin, 13 to 24% and 18 to 30%, respectively, suggesting that their production in MDP + Tc CM–activated monocytes is primarily independent of PGE_2 (Fig. 2, D and E). An expanded measurement of cytokines and chemokines in monocytes showed that Tc CM strongly amplified production of IL-8 (183-fold increase) in MDP-treated monocytes compared with MDP alone (fig. S3A). At the same time, IL-12 p40 and regulated on activation, normal T cell expressed and secreted (RANTES) were only modestly up-regulated by Tc CM (4.5- and 7-fold increase, respectively) (fig. S3, B and C). These data suggested that Tc CM signaling pathway strongly affects production of PGE_2, IL-1β, IL-6, and IL-8 and only modestly increases production of IL-12 p40 and RANTES.

Our previous data showed that IL-1β amplified PGE_2 production in human, LPS-primed monocytes (*22*). To determine whether IL-1β plays a role in MDP + Tc CM–induced production of PGE_2, caspase-1 inhibitor ZVAD was added to monocytes. ZVAD did not reduce PGE_2 up-regulated in monocytes by treatment with MDP and Tc CM (fig. S4A). In addition, the levels of *PTGS2* mRNA (which encodes COX-2 protein and is referred to as *COX2* hereafter) as a surrogate assay for PGE_2 were assayed in wild-type (WT) THP-1 Null cells and in THP-1 cells that do not have a functional NLRP3 inflammasome complex, THP1defNLRP3 and THP1defASC1 cells (fig. S4B). MDP alone and Tc CM alone minimally increased *COX2* mRNA expression in all THP-1 cells. In THP-1 Null, THP1defNLRP3, and THP1defASC1 cells, MDP + Tc CM treatment induced about 40-fold

increase in *COX2* mRNA compared with no treatment control; no differences were observed in the levels of *COX2* mRNA induction between MDP + Tc CM–activated THP-1 cells with and without functional NLRP3 inflammasome (fig. S4B). Together, these data suggest that CD3 bead–purified T cells produce a soluble factor that enhances production of PGE_2, IL-1β, IL-6, and IL-8 in MDP-activated monocytes in an IL-1β–independent fashion.

Tc CM promotes increase in *COX2* gene transcription but does not activate nuclear factor κB in MDP-treated monocytes

COX-2 and mPGES-1 are key enzymes in the biosynthesis of PGE_2 (*23*). To determine whether Tc CM up-regulates transcription of *COX2* and of *mPGES-1* genes in monocytes, *COX2* and *mPGES-1* mRNA expressions were assayed by reverse transcription quantitative polymerase chain reaction (RT-qPCR) (Fig. 3, A and B). MDP alone and MDP with Tc CM induced 12- and 325-fold increases in *COX2* mRNA, respectively, compared with no treatment control (Fig. 3A). In the case of *mPGES-1*, MDP and MDP with Tc CM induced 4- and 15-fold increases in mRNA expression, respectively (Fig. 3B). These data suggest that Tc CM primarily increases transcription of *COX2* and, to a lesser extent, transcription of *mPGES-1* mRNA in MDP-treated monocytes. CM from NS T cells that were incubated with CD3 microbeads overnight also increased *COX2* transcription in MDP-treated monocytes (fig. S5).

After recognition of MDP by NOD2, the receptor-interacting serine-threonine protein kinase-2 (RIP2 kinase) is recruited to the complex and activates nuclear factor κB (NF-κB) transcription factor (*24*, *25*). The promoter region of *COX2* gene contains multiple transcriptional regulatory sequences including two NF-κB sites (*26*). To investigate the role of NOD2/RIP2 signaling in our system, we assayed the levels of *COX2* and *mPGES-1* mRNA, PGE_2, and nuclear NF-κB p65 in monocytes activated with MDP and Tc CM in the absence or presence of the RIP2 kinase inhibitor erlotinib. Erlotinib reduced *COX2* mRNA by 80% in monocytes activated with MDP and Tc CM that correlated with reduction of PGE_2 production (Fig. 3, A and C). Similarly, IL-1β and IL-6 cytokines in MDP + Tc CM–activated monocytes were reduced by erlotinib by 50 to 80% (fig. S6, A to D). The level of *mPGES-1* mRNA was not affected by erlotinib in either MDP or MDP + Tc CM–treated cells (Fig. 3B). Nuclear extracts were prepared from monocytes and were immunoblotted for NF-κB p65 (p65) (Fig. 3, D and E, and fig. S7). Tc CM did not increase p65 compared with untreated monocytes. MDP alone and MDP + Tc CM induced about 7- and 10-fold increase in p65, respectively, compared with untreated monocytes (Fig. 3, D and E, and fig. S7). Nuclear p65 in monocytes treated with MDP with or without Tc CM was significantly reduced by erlotinib (Fig. 3, D and E, and fig. S7). These data suggest that Tc CM augmented *COX2* gene transcription via signaling pathway that does not require nuclear translocation of NF-κB p65.

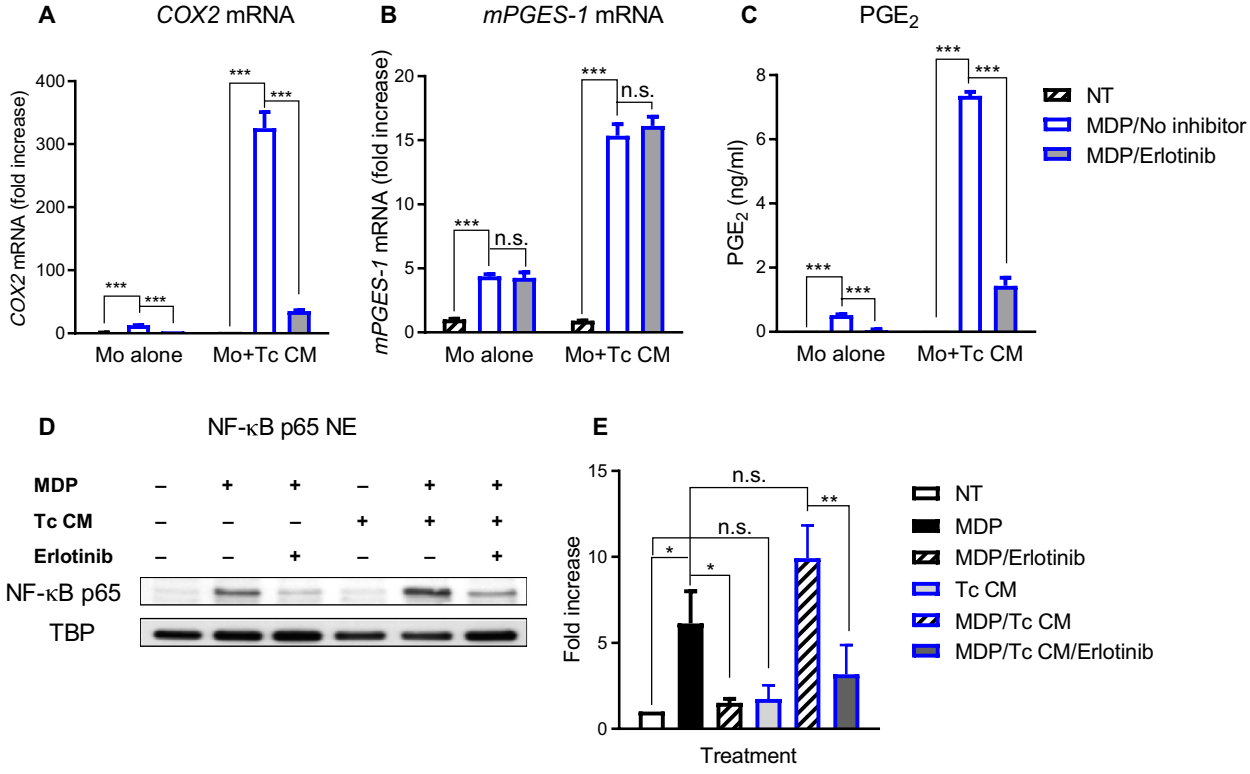

Fig. 3. Tc CM contributes to increased *COX2* gene transcription but not to activation and nuclear translocation of NF-κB. (**A** to **C**) RT-qPCR for *COX2* (A) and *mPGES-1* mRNA (B) and quantification of PGE_2 (C) in monocytes alone (Mo alone) or in monocytes incubated with Tc CM overnight (Mo + Tc CM) and either not treated (NT) or incubated with MDP in the absence (MDP/No inhibitor) or presence of erlotinib (MDP/Erlotinib). The C_t values for *COX2* (A) and *mPGES-1* mRNA (B) expression in monocytes were normalized using qPCR reactions with β-*actin* primers performed in the same samples. Data are mean fold increases in ΔC_t values over control (A and B) and means ± SD (C), each calculated from triplicate wells in a representative of three experiments performed with monocytes from individual donors. ***$P \leq 0.001$ and n.s., not significant, by two-tailed unpaired *t* test. (**D** and **E**) Western blot (D) and analysis (E) of NF-κB subunit p65 in nuclear extracts (NE) prepared from monocytes activated with MDP and Tc CM in the absence or presence of erlotinib for 3 hours. TATA-binding protein (TBP) was used as loading control for the nuclear extracts. Blot is from one donor of four (others are shown in fig. S7). Data are mean fold increases ± SEM; $n = 4$. *$P \leq 0.05$; **$P \leq 0.01$; and n.s., not significant ($P > 0.05$), by two-tailed unpaired *t* test.

PGE_2 production in MDP-treated monocytes is mediated by a Tc CM–induced increase in cytosolic [Ca^{2+}]

Calcium signaling plays a major role in LPS-induced activation of *COX2* gene transcription in gastric cancer cells (*27*). To investigate the role of calcium in our system, we used calcium chelator, 1,2-bis(2-aminophenoxy)ethane-*N*,*N*,*N*′,*N*′-tetraacetic acid tetrakis (acetoxymethyl ester) (BAPTA-AM), and inhibitors of phospholipase C (PLC) and of inositol 1,4,5-triphosphate receptor ($InsP_3R$) previously shown to prevent release of calcium from the endoplasmic reticulum to the cytosol in adenosine 5′-triphosphate–stimulated bone marrow–derived macrophages (*28*). PGE_2 production in monocytes activated with MDP and Tc CM was reduced about threefold by BAPTA-AM and was blocked by inhibitors of PLC and of $InsP_3R$, U73122 and 2-aminoethoxydiphenyl borate (2-APB), respectively (Fig. 4A). In a reverse experiment, a dose-dependent increase in PGE_2 production was observed in monocytes treated with MDP in the presence of the calcium ionophore ionomycin (0.1 to 1.0 μM), but not in monocytes treated with ionomycin alone (Fig. 4B). To confirm that Tc CM alone can increase cytosolic [Ca^{2+}], calcium flux was measured in monocytes. Tc CM but not NSTc CM (fig. S8) or MDP alone increased [Ca^{2+}] in monocytes, and there was no further increase in calcium flux when Tc CM was combined with MDP (Fig. 4C). These data suggested that Tc CM contains a factor that induces increase in cytosolic [Ca^{2+}] that delivers a second signal required for production of PGE_2 in monocytes activated with MDP.

GPIbα is a putative monocyte-activating factor in Tc CM

Before mass spectrometry (MS), Tc CM and NSTc CM were prepared from the same donor's PBMCs and were left untreated (neat) or were concentrated 18-fold [using 50-kDa molecular weight cutoff (MWCO) filters] and then added to monocytes in the presence of MDP. Tc CM induced about 31- and 34-fold more PGE_2 in MDP-treated monocytes compared with NSTc CM before and after concentration, respectively (table S2). No PGE_2-inducing activity was detected in the filtrates obtained after centrifugation of Tc CM or of NSTc CM, and treatment of concentrated Tc CM with CD26 peptidase reduced the PGE_2-inducing activity of Tc CM by 66% (table S2). These data suggested that Tc CM contains a protein with a molecular weight of ≥50 kDa that enhances production of PGE_2 in MDP-treated monocytes.

For MS analysis, serum-free Tc CM and NSTc CM were prepared from the same donor's PBMCs and were concentrated 18-fold. The PGE_2-inducing activity of concentrated Tc CM increased 29-fold compared with neat Tc CM and was 13-fold higher than PGE_2-inducing activity of concentrated NSTc CM (Table 1). The MS analysis of concentrated CM revealed several proteins that were present at higher amounts in Tc CM compared with NSTc CM; of those, the highest difference was noted for GPIbα that was detected at a 14-fold higher level in Tc CM compared with NSTc CM (table S3).

GPIbα protein is constitutively shed from human platelets (*29*) that are present in large quantities in blood, about 150 billion to 400 billion platelets per 1 liter of blood in a healthy adult. To confirm that T cells used to obtain CM were not contaminated with platelets, NS T cells, CD3 bead–purified T cells, and purified platelets in control were assayed by flow cytometry using antibodies against the platelet marker CD41a (fig. S9). Platelets were 99.9% $CD41a^+$. At the same time, only about 0.3% of $CD41a^+$ platelets were detected in NS T cells and in CD3 bead–purified T cells (fig. S9). In addition, flow cytometry cell sorting was used to purify $CD41a^-CD45^+CD4^+$ and $CD41a^-CD45^+CD8^+$ cells (fig. S10). The sort-purified $CD4^+$ and $CD8^+$ cells were 100% positive for CD3 T cell marker (fig. S10). Sort-purified $CD4^+$ and $CD8^+$ T cells were mixed together and were cultured overnight with CD3 beads (fig. S11). CM from CD3 bead–treated sorted cells induced about 10- and 20-fold increases in *COX2* mRNA and PGE_2 compared with MDP treatment alone, respectively, which was in the same range as *COX2* mRNA and PGE_2 increases induced by CM from CD3 bead–purified T cells isolated from the same donor's PBMC (fig. S11).

To confirm that T cells produce endogenous GPIbα after treatment with CD3 beads, *GPIbα* mRNA expressions were assessed by RT-qPCR in total RNA extracted from NS T cells and from CD3 bead–purified T cells cultured overnight (Fig. 5A). CD3 bead–purified T cells showed about a sixfold increase in *GPIbα* mRNA compared with NS T cells (Fig. 5A, two donors). In parallel, Tc CM and NSTc CM were concentrated and were immunoblotted for GPIbα using SZ2 monoclonal antibody (mAb) (*30*) along with positive

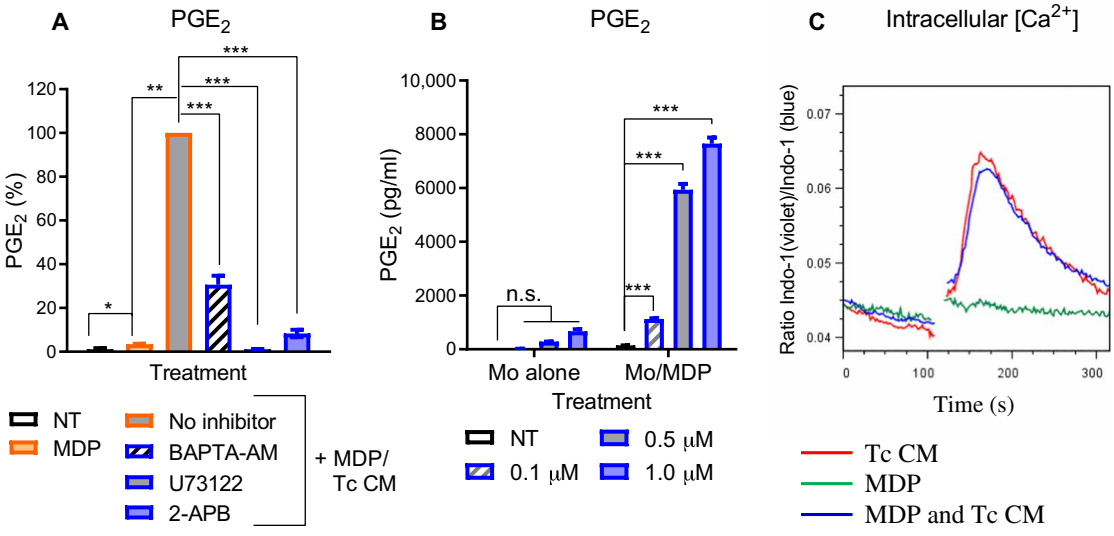

Fig. 4. Increase in intracellular [Ca^{2+}] is required for production of PGE_2 in monocytes. (**A**) PGE_2 quantification in monocytes that were not treated (NT), incubated with MDP alone, or incubated with MDP and Tc CM (MDP/Tc CM) either alone (No inhibitor) or in the presence of BAPTA-AM, U73122, or 2-APB. Data are means ± SD from triplicate wells in a representative of three experiments. *$P \leq 0.05$, **$P \leq 0.01$, and ***$P \leq 0.001$, by two-tailed unpaired *t* test. (**B**) PGE_2 quantification in monocytes either unperturbed (Mo alone) or incubated with MDP (Mo/MDP) and either not treated (NT) or treated with 0.1, 0.5, or 1.0 μM ionomycin. Data analysis and *N* as described in (A). (**C**) Representative Indo-1 fluorescence time traces in monocytes after treatment with MDP, Tc CM, or MDP and Tc CM. The ratio of mean Indo violet/Indo blue emission values (405 nm:485 nm) indicates changes in free intracellular [Ca^{2+}] over time. Traces are from a representative of three experiments.

controls: platelet cell extracts and recombinant GPIbα (rGPIbα) protein (Fig. 5B). The molecular weight of GPIbα in Tc CM was 120 to 125 kDa and was slightly lower than 135-kDa GPIbα detected in platelet extracts (Fig. 5B). Densitometry of GPIbα bands in Tc CM and in rGPIbα showed that the neat Tc CM from donors 1 and 2 contained GPIbα (3.3 and 6.2 ng/ml, respectively; Fig. 5B).

Table 1. PGE_2-inducing activity of serum-free Tc CM and NSTc CM used for MS. Quantification of PGE_2 in monocytes treated with MDP in the presence of conditioned medium (CM) prepared from CD3 bead–isolated T cells (Tc CM) or from negatively selected T cells (NSTc CM) cultured overnight in serum-free Expi293 medium.

CM*	PGE_2 ± SD (pg/ml)†		Fold increase‡
	Tc CM	NSTc CM	
Neat	2,309.0 ± 4.4	250.0 ± 8.3	9.2
Concentrated	66,769.8 ± 14,258.8	5,128.0 ± 1,784.0	13.0

*Tc CM and NSTc CM were left untreated (Neat) or were concentrated using a 50-kDa MWCO centrifugal filter (Concentrated). †Monocytes were treated with MDP in the presence of Tc CM Neat or Concentrated or with MDP in the presence of NSTc CM Neat or Concentrated overnight. Monocyte cell culture supernatants were assayed for PGE_2 production. Data are shown as means ± SD from triplicates. ‡Fold increase was calculated for PGE_2 production in monocytes incubated with MDP and Tc CM versus MDP and NSTc CM. Representative of three experiments.

ADAM17 and ADAM10 metalloproteases are both expressed by T cells and are involved in shedding of several transmembrane receptors, cytokines, and adhesion molecules (*31*). To determine whether GPIbα in Tc CM is shed from T cells, the inhibitor of metalloprotease, matrix metalloproteinase 8 inhibitor I (M8I) (*32*), and dimethyl sulfoxide (DMSO) in control were added to CD3 bead–purified T cells during overnight cell culture. Tc CM and Tc CM prepared in the presence of M8I (Tc CM/M8I) were immunoblotted for GPIbα and were assayed for PGE_2-inducing activity (Fig. 5, C and D). Densitometry showed that, for donors 1 and 2, Tc CM contained GPIbα (2.0 and 4.9 ng/ml, respectively), and the GPIbα bands were reduced in Tc CM/M8I (Fig. 5C). Tc CM/M8I induced about 70% less PGE_2 in monocytes compared with Tc CM (Fig. 5D). These data further supported the notion that T cells activated with CD3 microbeads increased *GPIbα* mRNA and shed GPIbα protein during overnight culture via M8I-sensitive metalloprotease. Although platelets constitutively shed GPIbα during incubation, they failed to induce increase in PGE_2 production in MDP-treated monocytes, suggesting that the T cell–derived and not platelet-derived GPIbα augment MDP/NOD2-initiated signaling pathway in monocytes (fig. S12).

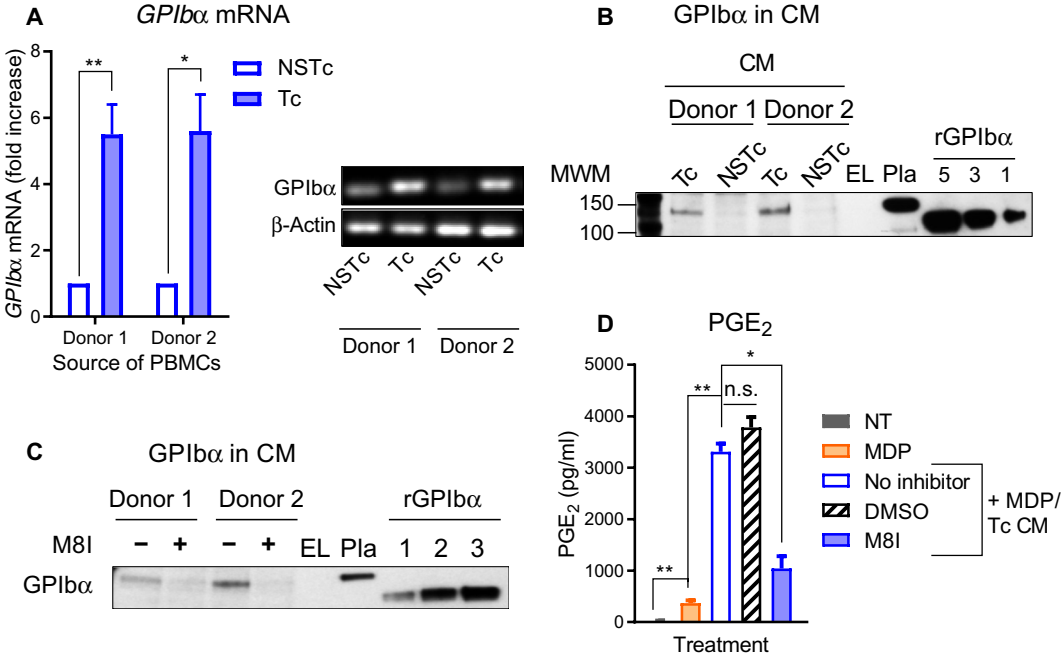

Fig. 5. T cells isolated using CD3 beads expressed increased levels of *GPIbα* mRNA and shed GPIbα protein in CM. (**A**) Left: RT-qPCR for GPIbα mRNA in CD3 bead–purified T cells (Tc) and in negatively selected T cells (NSTc) from donors 1 and 2 cultured overnight. The C_t values for *GPIbα* mRNA expressions in T cells were normalized using qPCR reactions with β-*actin* primers performed in the same samples. Data are fold increases from triplicate wells. *$P \leq 0.05$ and **$P \leq 0.01$, by two-tailed unpaired *t* test. Right: Agarose gels for GPIbα and β-actin transcripts. Representative of two experiments. (**B**) Western blot of 3.5-fold concentrated CM from CD3 bead–purified T cells (Tc) and from negatively selected T cells (NSTc) from donors 1 and 2 (25 μl of concentrated CM per lane), total cell extracts from platelets (Pla) (0.1 μg of total protein per lane), and rGPIbα (5, 3, and 1 ng of protein per lane). MWM, molecular weight markers; EL, empty lane. Data are representative of three experiments. (**C**) Western blot of 18-fold concentrated CM from CD3 bead–purified T cells cultured in the absence or in the presence of M8I (7.5 μl of concentrated CM per lane), platelet extracts (0.1 μg of total protein per lane), and an rGPIbα protein (1, 3, and 5 ng of protein per lane). Data are representative of three experiments. (**D**) Quantification of PGE_2 in monocytes not treated (NT) or incubated with MDP alone (MDP), with MDP and Tc CM alone (No inhibitor), or in the presence of M8I or DMSO in control. Data are means ± SD from triplicate wells from two experiments. *$P \leq 0.05$; **$P \leq 0.01$; and n.s., not significant, by two-tailed unpaired *t* test.

T cell–derived GPIbα delivers a second signal to monocytes via Mac-1 integrin

Mac-1 integrin (αM/β2, CD11b/CD18) is a receptor for a platelet-associated GPIbα (*33*). To determine whether Mac-1 recognizes T cell–derived soluble GPIbα, anti-GPIbα and anti-CD11b mAbs or normal mouse immunoglobulin G1 (IgG1) in control was added to monocytes. *COX2*, *IL1B*, and *IL6* mRNA and PGE_2, IL-1β, and IL-6 proteins were assayed in monocytes and in cell culture supernatants, respectively. mAb to GPIbα reduced expression of *COX-2* mRNA and PGE_2 production by 80 and 60%, respectively, and anti-CD11b mAbs reduced both by 80% compared with monocytes treated with MDP and Tc CM (Fig. 6, A and B). Similarly, anti-GPIbα mAb reduced *IL1B* and *IL6* mRNA by 80% and IL-1β and IL-6 protein by 53 and 35%, respectively (Fig. 6, C to F). mAb to CD11b reduced *IL1B* and *IL6* mRNA by 80% and IL-1β and IL-6

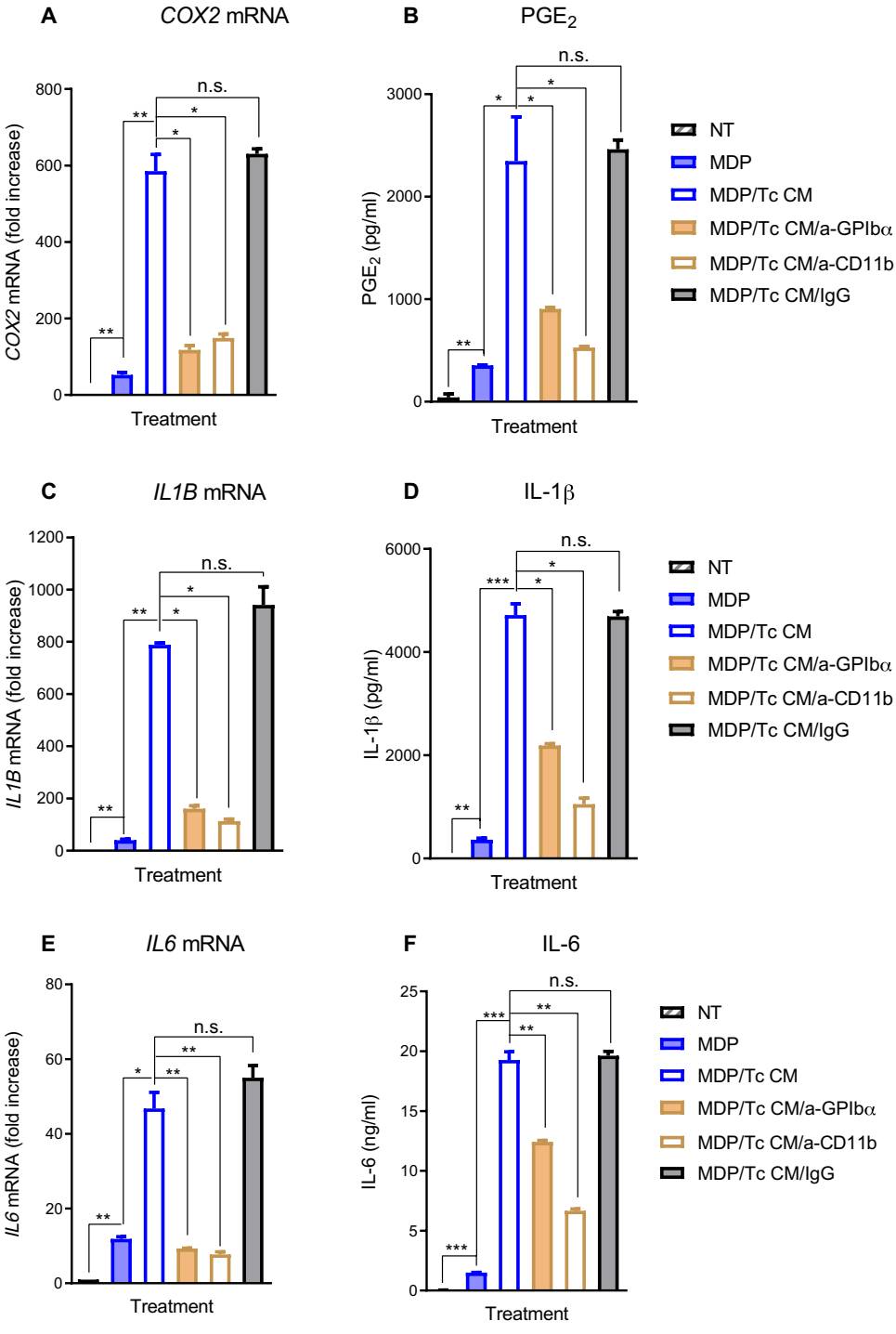

Fig. 6. Antibodies to GPIbα and CD11b reduced *COX2*, *IL1B*, and *IL6* mRNA expression and PGE_2, IL-1β, and IL-6 protein secretion in monocytes activated with MDP and Tc CM. (**A** to **F**) Quantification of *COX2* (A), *IL1B* (C), and *IL6* mRNA (E) expression and quantification of PGE_2 (B), IL-1β (D), and IL-6 (F) in monocytes treated with MDP alone or with MDP and Tc CM in the absence or presence of mAbs to GPIbα or Mac-1 (CD11b) or mouse IgG1 in control. The C_t values (A, C, and E) were normalized to that of β-*actin* performed in the same samples. Data are means ± SD from triplicate wells in a representative of three experiments. $^*P \leq 0.05$; $^{**}P \leq 0.01$; $^{***}P \leq 0.001$; and n.s., not significant, by two-tailed unpaired *t* test.

protein by 80 and 63%, respectively (Fig. 6, C to F). As a control, mouse IgG1 did not reduce *COX2*, *IL1B*, and *IL6* mRNA or PGE_2 and IL-1β/IL-6 proteins up-regulated by MDP and Tc CM (Fig. 6, A to F).

In addition to antibody-mediated blocking of Mac-1 in monocytes, we tested the effect of CD11b gene silencing in THP-1 cells that were transfected with *CD11b* small interfering RNA (siRNA) or with control siRNA. The efficiency of *CD11b* gene silencing was confirmed by Western blotting and was 85% (Fig. 7A). MDP/Tc CM induced about 50- and 150-fold increases in *COX2* and in *IL1B* mRNA in THP-1 cells transfected with control siRNA, respectively. Transfection with CD11b siRNA resulted in two- and threefold reduced levels of *COX2* and of *IL1B* mRNA, respectively, in THP-1 cells activated with MDP and Tc CM (Fig. 7, B and C).

The role of Mac-1 integrin in up-regulation of cytosolic $[Ca^{2+}]$ by Tc CM in human monocytes

Antibody-mediated cross-linking of Mac-1 in neutrophils and in monocytic cell lines, THP-1 and HL-60, was shown to increase cytosolic $[Ca^{2+}]$ (*34*, *35*). To determine whether, in our system, Tc CM increased calcium through Mac-1, monocytes were preincubated with anti-CD11b mAb or with normal mouse IgG1 and were subjected to calcium flux analysis (Fig. 7D). Pretreatment of monocytes with anti-CD11b mAb but not with control IgG1 completely blocked Tc CM–induced increase in cytosolic $[Ca^{2+}]$ (Fig. 7D).

Mice deficient in Mac-1 expression demonstrate lower *Cox2* mRNA induction after MDP administration

To determine whether Mac-1 plays a role in MDP-induced increase in PGE_2 in vivo, *Cox2* mRNA expressions were measured in the livers and spleens of CD18 knockout (KO) and αM KO mice that lack expression of Mac-1 and in WT control mice after administration of MDP or PBS (Fig. 7E and fig. S13). *Cox2* C_t values in the spleen and liver in all three groups of mice were lower at 2 hours after treatment with MDP compared with PBS treatment (fig. S13). However, the fold increase in *Cox2* mRNA expression after MDP treatment was

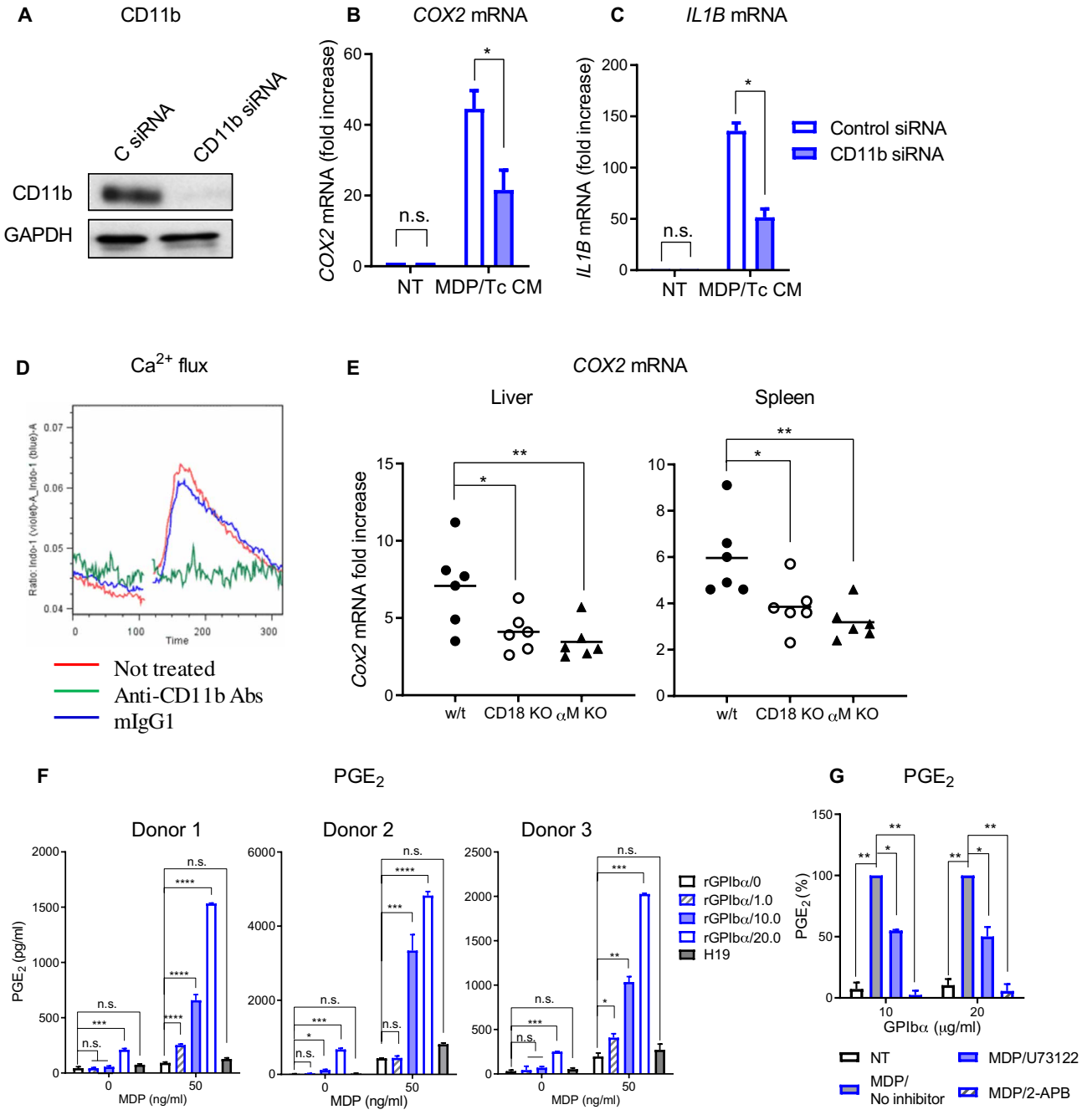

Fig. 7. Signaling through Mac-1 receptor is required for PGE_2 production in MDP-activated monocytes. (**A**) Western blot for CD11b in THP-1 cells transfected with control or with siRNA targeting *CD11b*. Representative of two experiments. GAPDH, glyceraldehyde-3-phosphate dehydrogenase. (**B** and **C**) RT-qPCR for *COX2* (B) and *IL1B* (C) expression in THP-1 cells transfected with control siRNA or *CD11b* siRNA and either not treated (NT) or treated with MDP and Tc CM (MDP/Tc CM). Data are mean fold increases ± SD over control (without MDP and Tc CM treatment) in triplicate wells in a representative of three experiments. *$P \leq 0.05$ and n.s., not significant, by two-tailed unpaired *t* test. (**D**) Ca^{2+} transients in response to Tc CM were recorded in monocytes untreated or pretreated with antibodies to CD11b or with mouse IgG1 (mIgG1). The Indo-1 ratio of emission intensities (405 nm:485 nm) over time is presented. Representative of three experiments. (**E**) Quantification of mouse *Cox2* mRNA in the liver and spleen of WT (w/t), CD18 KO, and αM KO mice at 2 hours after inoculation of MDP. The data show fold increases in *Cox2* mRNA ΔC_t values in mice that received MDP (six mice per group) over average *Cox2* ΔC_t values in mice that received PBS (four mice per group); fold increase for each mouse and means calculated for the groups of mice are shown. *$P \leq 0.05$ and **$P \leq 0.01$, by two-tailed unpaired *t* test. (**F**) Quantification of PGE_2 in monocytes (Donor 1, Donor 2, and Donor 3) not treated (rGPIbα/0) or treated with rGPIbα at 1, 10, or 20 μg/ml or with H19 peptide (20 μg/ml) alone (MDP 0) or in the presence of MDP at 50 ng/ml. Data are means ± SD from triplicate wells. *$P \leq 0.05$, **$P \leq 0.01$, ***$P \leq 0.001$, and ****$P \leq 0.0001$, by two-tailed unpaired *t* test. (**G**) PGE_2 quantification in monocytes incubated with rGPIbα (10 and 20 μg/ml) alone [not treated (NT)], with rGPIbα in the presence of MDP alone (No inhibitor), or with rGPIbα and MDP in the presence of U73122 or 2-APB. Data are means ± SD from two independent experiments. *$P \leq 0.05$ and **$P \leq 0.01$, by two-tailed unpaired *t* test.

significantly higher in WT mice compared with CD18 KO or αM KO mice (Fig. 7E), confirming that Mac-1 signaling contributes to MDP-induced *Cox2* transcription in vivo.

PGE_2 production in monocytes activated with MDP and rGPIbα is sensitive to inhibitors of calcium pathway

To confirm the role of GPIbα in the induction of PGE_2 in monocytes, monocytes were treated with MDP alone, with rGPIbα alone (1.0, 10.0, and 20 μg/ml), with MDP in the presence of rGPIbα, or with a negative control peptide H19 alone or in combination with MDP (Fig. 7F and fig. S14A; three donors) (*36*). PGE_2 in monocytes treated with rGPIbα alone was at background levels (not treated monocytes) or was slightly elevated at the highest dose only (Fig. 7F). Ten and 20 μg/ml of rGPIbα induced 7- to 15-fold and 14- to 33-fold increase in PGE_2 production in monocytes treated with 50 or 5 ng/ml of MDP, respectively, compared with MDP treatment alone (Fig. 7F and fig. S14, A to C). H19 peptide added to MDP did not alter the levels of PGE_2 in monocytes compared with MDP treatment alone (Fig. 7F and fig. S14B). rGPIbα-induced PGE_2 production in MDP-treated monocytes was reduced by inhibitors of calcium pathway, PLC (U73122) and $InsP_3R$ (2-APB) (50 and 90%, respectively) (Fig. 7G). In addition to PGE_2, rGPIbα induced significant increase in production of IL-1β and IL-6 in MDP-treated monocytes (fig. S14, D and E). No further up-regulation of nuclear NF-κB p65 was detected in monocytes treated with rGPIbα over p65 in the nuclear extracts of MDP-treated monocytes, suggesting that rGPIbα up-regulated PGE_2 but did not enhance activation of NF-κB (fig. S15).

Together, our studies demonstrated that T cells treated with CD3 microbeads up-regulate GPIbα mRNA and shed GPIbα protein and that cooperation between two signaling pathways, GPIbα/Mac-1 and MDP/NOD2, is required for production of PGE_2 and proinflammatory cytokines IL-1β, IL-6, and IL-8 in MDP-activated monocytes.

DISCUSSION

The key role of PGE_2 in inflammatory responses in the tissues has been well established: PGE_2 was shown to promote vascular permeability to facilitate the tissue influx of neutrophils, macrophages, and mast cells from the blood stream leading to swelling and edema at the site of infection and to stimulate sensory nerves to increase the pain response and promote fever (*37*). Our previous studies with human monocytes activated with TLR agonists suggested that circulating monocytes may serve as a major source of PGE_2 (*21*). In this study, we investigated the mechanism of PGE_2 production in monocytes in response to a NOD2 agonist, MDP. On the basis of our data, we suggest that production of proinflammatory substances such as PGE_2, IL-1β, IL-6, and IL-8 cytokines in monocytes activated with MDP adjuvant requires an additional signal provided by T cell–derived GPIbα (Fig. 8). In this model, signaling initiated by MDP/NOD2/RIP2 complex activates the transcription factor NF-κB (*24*, *25*, *38*) and is augmented by T cell–derived GPIbα that triggers Mac-1 integrin on monocytes, which increases cytosolic calcium that facilitates subsequent gene transcription (Fig. 8).

Administration of MDP in vivo (in rabbits and in humans) was clearly associated with substantial reactogenicity including an increase in body temperature. Monocytes express NOD2 (*24*); however, in our studies, high doses of MDP alone did not induce PGE_2 in human monocytes, suggesting that engagement of NOD2 by MDP was insufficient. In search for the source of missing signal(s), we found that addition of Tc CM to MDP-treated monocytes induced up to 30-fold increase in the levels of PGE_2 and of IL-1β/IL-6. A possibility that PGE_2 in monocytes was induced by IL-1β (*39*) was ruled out by showing that ZVAD did not reduce PGE_2 in monocytes and that MDP + Tc CM treatment induced similar increases in *COX2* mRNA in WT and in *NLRP3*$^{-/-}$ and *ASC1*$^{-/-}$ THP-1 cells. In addition, MDP + Tc CM induced substantial increase in IL-8 and minimal increase in IL-12 p40 and RANTES in MDP-treated monocytes. Therefore, Tc CM augments transcription of cytokines that are controlled by NF-κB p65 (IL-1β, IL-6, and IL-8) and not by c-Rel protein (IL-12 p40 and RANTES) or chemokines (RANTES) that require interferon regulatory transcription factors (IRF-3 or IRF-8) that cooperate with NF-κB (*40*–*43*).

GPIbα protein was identified in CM from CD3 bead–purified T cells but not in CM from NS T cells by MS analysis. The presence of GPIbα in Tc CM was unexpected. GPIbα is abundantly expressed on the platelet surface where it serves as a receptor for von Willebrand factor (VWF) and plays an important role in thrombosis, thrombocytopenia, and inflammation (*44*, *45*).The platelet-associated GPIbα

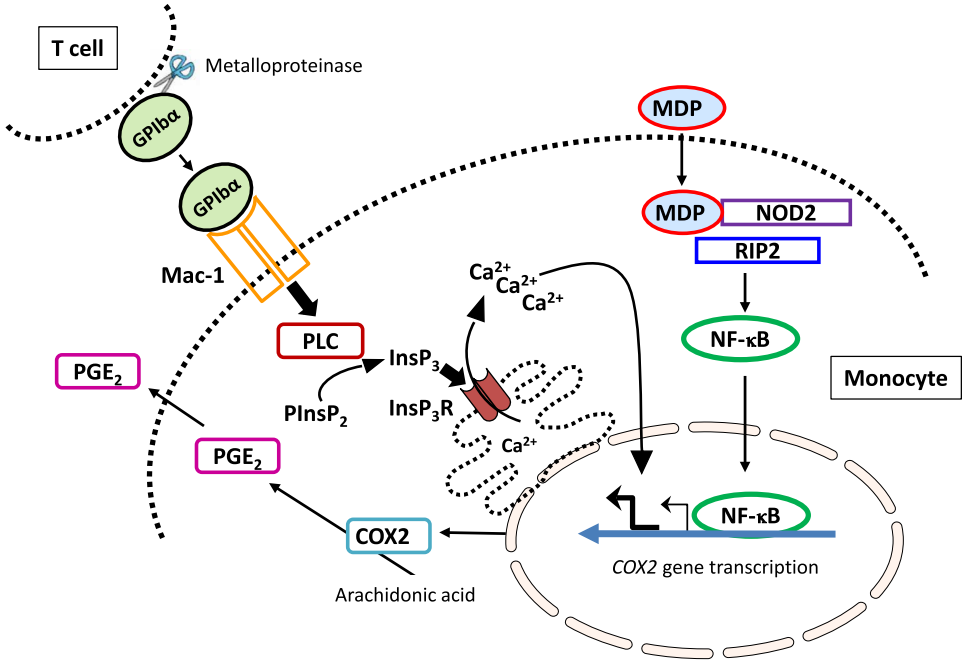

Fig. 8. Model of PGE_2 production in monocytes activated with MDP and Tc CM. MDP alone induced nuclear NF-κB and low levels of *COX2* transcription and PGE_2 production. CD3 bead–activated T cells shed GPIbα protein by the activity of metalloprotease. Triggering of Mac-1 in monocytes by T cell–derived GPIbα activates PLC/$InsP_3$/$InsP_3R$ pathway and induces release of calcium from the endoplasmic reticulum. Increase in cytosolic calcium provides a second signal essential for increased *COX2* transcription and subsequent production of PGE_2 in MDP-activated monocytes.

is a 145-kDa type I transmembrane protein that contains an extracellular ligand-binding domain with leucine-rich repeats (LRRs) and a sialomucin region, a transmembrane helix, and a short cytoplasmic tail (*46*). The 135-kDa ligand-binding domain of GPIbα, known as glycocalicin, is constitutively shed from platelets, and the intact and proteolytic fragments of GPIbα extracellular domain are detectable by Western blot on extracts of circulating platelets (*29*, *47*). Besides VWF, GPIbα binds multiple components of the coagulation cascade, the membrane glycoproteins P-selectin and Mac-1 (*33*, *48*). Platelets did not up-regulate PGE_2 in MDP-treated monocytes when cultured in transwell plates, suggesting that GPIbα produced by semiactivated T cells is functionally different from platelet-derived GPIbα. The reason for a slightly smaller GPIbα fragment present in Tc CM (120 to 125 kDa) compared with GPIbα in platelet extracts (135 kDa) is not clear. In addition to the ADAM17 cleavage site, other sites for proteolytic cleavage were identified in the GPIbα extracellular domain that may explain a slightly smaller fragment of T cell–derived GPIbα (*49*).

It is important to note that the PGE_2-inducing activity of Tc CM was reproduced by human embryonic kidney (HEK) 293–derived rGPIbα. Microgram quantities of rGPIbα induced similar increases in PGE_2 production in MDP-treated monocytes as were induced by Tc CM calculated to contain nanogram quantities of GPIbα. It is not clear whether the difference in the activity is related to differences in the primary sequences or glycosylation pattern in T cells versus platelet-derived GPIbα or that Tc CM may contain other substances that contribute to PGE_2-inducing activity of soluble GPIbα.

Mac-1 is expressed by monocytes, macrophages, and Kupffer cells, and it serves as a receptor for GPIbα, fibrinogen, complement fragment C3bi, coagulation factor X, heparin, and intercellular adhesion molecule–1 (*33*, *50*). In our experiments, anti-GPIbα (HIP1) mAbs that bind to a conformational epitope within the first three LRRs in the ligand-binding domain of the GPIbα (*30*) reduced production of PGE_2 and of IL-1β and IL-6 in monocytes. Thus, our data agree with a previous study that identified binding sites for Mac-1 in the LRR domain of GPIbα (*33*).

Relatively small increases in *Cox2* mRNA expression observed in the liver and spleen of WT mice after injection of MDP may be attributed to the reported low sensitivity of mice to the pyrogenic effect of MDP compared with rabbits: MDP administered intravenously at 25 mg/kg was not reactogenic in mice, yet MDP administered at 30 to 50 μg/kg induced pyrogenic response in rabbits (*51*, *52*). The increase in *Cox2* mRNA expression after MDP treatment was substantially smaller in mice that lack Mac-1 expression compared with WT mice, suggesting that Mac-1 signaling contributes to up-regulation of *Cox2* in MDP-treated animals.

Signaling initiated by engaged integrin receptors can amplify or dampen specific immune response from other receptors such as tyrosine kinases, heterotrimeric GTP-binding protein–coupled receptors, and cytokine receptors (*53*). Mac-1 engaged by T cell–derived GPIbα can enable monocytes to mount a strong inflammatory response to a weak signal from NOD2 receptor triggered by MDP adjuvant. Thus, the local cell environment can markedly affect the outcome of the innate response to an adjuvant in the context of vaccine-antigen–activated T cells. Our findings indicate that a T cell–monocyte nexus might be further explored to investigate the biological activity of novel vaccine adjuvants and to better understand systemic adverse reactions in clinical trials.

MATERIALS AND METHODS

Cells and cell treatments

Human buffy coats, human monocytes isolated using counterflow centrifugal elutriation (*54*), and human platelets (all from healthy donors) were obtained from the Department of Transfusion at the National Institutes of Health (Bethesda, MD). Human PBMCs were purified from buffy coats by Ficoll-Paque PLUS gradient centrifugation (GE Healthcare Bio-Sciences). In some experiments, monocytes were removed from PBMCs using CD14 microbeads (PBMC-Mo) (Miltenyi Biotec). T cells were purified from PBMCs using CD3 microbeads; NS T cells were purified from PBMCs using Pan T cell isolation kit according to the manufacturer's instructions (Miltenyi Biotec). T cells isolated using CD3 microbeads or using Pan T isolation kit were 99% pure, as verified by flow cytometry using anti-CD3 mAb.

CM was prepared from CD3 bead–purified T cells (Tc CM) or from NS T cells (NSTc CM) cultured at 15×10^6/ml in RPMI 1640 medium with 1% fetal bovine serum (FBS) at 37°C and 5% CO_2 overnight. In some experiments, metalloproteinase inhibitor M8I at 80 μM (EMD Millipore) or DMSO was added during overnight incubation of CD3 bead–purified T cells. In some experiments, CM was obtained from NS T cells cultured at 15×10^6/ml with CD3 microbeads (0.3 or 3.0 μl/ml) added directly to cell culture wells in RPMI 1640 medium with 1% FBS at 37°C overnight.

PBMCs, PBMC-Mo, or monocytes were cultured at 15×10^6 cells/ml with MDP at 50 or 500 ng/ml in a complete RPMI 1640 medium with 10% FBS and supplements in 96-well or 24-well plates, respectively, at 37°C and 5% CO_2 overnight. In some experiments, monocytes were cocultured with T cells in the same well or in separate chambers of a transwell system (monocytes in the bottom chamber) at a 7:3 ratio of monocytes to T cells or were cultured in the presence of Tc CM or NSTc CM at 7:3 volume ratio, with HEK293 cell line–derived recombinant human GPIbα protein (Sino Biological, catalog no. 11765-H08H, lot 1811), or with H19 peptide corresponding to residues 340 to 357 in the γ chain of fibrinogen that does not bind Mac-1 (20 μg/ml) (*36*). In some experiments, monocytes were activated with LPS (Enzo Life Sciences) or with ionomycin (Tocris Bioscience). In some experiments, monocytes were preincubated with the following reagents for 1 hour before adding MDP and Tc CM: erlotinib (40 μM) (Santa Cruz Biotechnology); 2-APB (50 μM) and U73122 (25 μM) (all from EMD Millipore); BAPTA-AM (50 μM) (Tocris Bioscience); indomethacin (Sigma Chemical Co.); ZVAD (10 μg/ml; Bachem Americas); or anti-GP1bα/CD42b IgG1 mAb clone HIP1 (catalog no. 14-0429-82), anti-CD11b IgG1 mAb clone CBRM1/5 (catalog no. 14-0113-81), or IgG1 kappa (catalog no. 16-4714-82) at 4 μg/ml (all from Thermo Fisher Scientific).

In some experiments, platelets (15×10^6/ml) were cultured with MDP at 500 ng/ml alone or were cocultured with monocytes (15×10^6 cells/ml) in separate chambers of a transwell system, monocytes in the bottom chamber at a 7:3 v/v ratio of monocytes to platelets in complete RPMI 1640 medium with 10% FBS and supplements at 37°C and 5% CO_2 overnight.

THP1defNLRP3, THP1defASC1, and THP-1 Null (control) cells (InvivoGen) were seeded in 24-well plate at 2×10^5 cells per well in complete RPMI 1640 medium with 10% FBS and supplements and were incubated with phorbol myristate acetate (PMA; 100 ng/ml) for 24 hours at 37°C and 5% CO_2. The next day, PMA-activated THP-1 cells were treated with MDP and Tc CM using the same conditions that were used in monocyte cell cultures. The study received an exempt status by the RIHS Committee at Center for Biologics

Evaluation and Research (CBER), U.S. Food and Drug Administration (FDA).

MS analysis of concentrated CMs and database search

Concentration of CM

Tc CM and NSTc CM from the same donor's PBMCs were concentrated using a 50-kDa MWCO Amicon Ultra-0.5 Centrifugal Filter Unit (EMD Millipore). Concentrate and flow-through (filtrate) were collected. Concentrated Tc CM was incubated with CD26 peptidase (0.4 U/ml) (Thermo Fisher Scientific) at 37°C for 2 hours, followed by incubation with 2 mM diprotin A (Sigma) at 37°C for 15 min (to inactivate peptidase activity). Concentrate and filtrate from Tc CM and NSTc CM and CD26-treated concentrated Tc CM were tested for induction of PGE_2 in MDP-treated monocytes.

Sample preparation for MS

CD3 bead–purified T cells and NS T cells from the same donor's PBMCs washed five times in serum-free PBS were cultured at 15×10^6 cells/ml in serum-free Expi293 Expression Medium (Thermo Fisher Scientific) at 37°C overnight. Tc CM and NSTc CM were collected and concentrated 18-fold using a 50-kDa MWCO Amicon Ultra-0.5 Centrifugal Filter Unit (EMD Millipore), and protein concentrations of Tc CM or NSTc CM were determined by BCA protein assay kit (Thermo Fisher Scientific).

Concentrated Tc CM and NSTc CM were analyzed by liquid chromatography–tandem MS (LC/MS/MS) using Thermo Fisher Scientific Ultimate LC and Fusion Orbitrap MS. Typical settings for quantitative proteomics at FDA's Facility for Biotechnology Resources were used in the analysis (*55*). Proteome Discoverer 1.4 (Thermo Fisher Scientific) was used to match MS/MS spectra to peptides using the Swiss-Prot human database. The parameter settings were previously reported (*56*).

Measurement of cytosolic $[Ca^{2+}]$ in human monocytes

Monocytes (10^7/ml) were labeled with Indo-1AM (2 μg/ml) (Molecular Probes) in loading buffer (Hanks' balanced salt solution with $CaCl_2$ and $MgSO_4$, 10 mM Hepes, and 1% FBS) with 1 mM probenecid (Thermo Fisher Scientific) at 37°C for 30 min. Labeled monocytes were washed and resuspended to 7.5×10^6 cells/ml in loading buffer. In some experiments, Indo-1–loaded cells were incubated with anti-CD11b mAb clone CBRM1/5 (8 μg/ml) (catalog no. 14-0113-81) or IgG1 kappa (catalog no. 16-4714-82) (both from Thermo Fisher Scientific) at room temperature for 30 min. Each Indo-1–loaded probe (400 μl) was warmed up at 37°C for 4 min immediately before signal acquisition. Fluorescence signals from labeled monocytes were acquired on LSRFortessa flow cytometer (BD Biosciences) using 525/50 band-pass with 450 long-pass filters for Indo-1 blue and 450/20 band-pass filter for Indo-1 violet. Baseline fluorescence signal was acquired for 1 min, after which 100 μl of Tc CM or NSTc CM or MDP (500 ng/ml) was added, and data were acquired for two more minutes. Changes in the intracellular calcium concentration were registered as a shift in the Indo-1 emission peak from 485 nm (unbound Indo) to 405 nm (calcium-bound Indo). Data were analyzed with FlowJo 7.6.5 software (TreeStar).

Measurements of PGE_2 by fluorescence resonance energy transfer assay and of IL-1β, IL-6, IL-8, RANTES, and IL-12 p40 cytokines by enzyme-linked immunosorbent assay

Cell culture supernatants from PBMCs, monocytes, and platelets were collected and assayed for PGE_2 by fluorescence resonance energy transfer (FRET) assay using PGE_2 Homogeneous Time-Resolved Fluorescence assay (HTRF) Kit (Cisbio Bioassays) and Novostar plate reader (BMG Labtech) as previously described (*21*). PGE_2 concentrations were calculated using four-parameter logistic fit using Origin software application (OriginLab). The detectable PGE_2 range was from 10 to 5000 pg/ml. IL-1β, IL-6, IL-8, RANTES, and IL-12 p40 cytokines were measured in the monocyte cell culture supernatants using human Quantikine enzyme-linked immunosorbent assay (ELISA) kits (R&D Systems) and Synergy2 Multi-Mode plate reader (BioTek Instruments).

qPCR for *COX2*, *mPGES-1*, *IL1B*, *IL6*, and *GP1bα* mRNA

Cells were lysed in RLT buffer (RNeasy; QIAGEN) and homogenized with QIAshredder (QIAGEN), and total RNA was isolated according to the manufacturer's protocol. Complementary DNAs (cDNAs) were prepared using a Reverse Transcriptase SuperScript VILO (Life Technologies). qPCR was performed using Power SYBR Green (Applied Biosystems) and a QuantStudio 6 Flex Real-Time PCR system (Applied Biosystems). The following primer pairs were used: *COX2* (sense, 5′-GAATCATTCACCAGGCAAATTG-3′ and antisense, 5′-TTTCTGTACTGCGGGTGGAAC-3′), *mPGES-1* (sense, 5′-CTGCTGGTCATCAAGATGTACG-3′ and antisense, 5′-GGTTAGGACCCAGAAAGGAGT-3′), *IL1B* (sense, 5′-TGATGGCTTATTACAGTGGCAAT-3′ and antisense, 5′-AGAGGGCAGAGGTCCAGG-3′), *IL6* (sense, 5′-AGAGGCACTGGCAGAAAACA-3′ and antisense, 5′-TCACCAGGCAAGTCTCCTCA-3′), *GP1bα* (sense, 5′-GTCGAGTGGCACCCTAGAAG-3′ and antisense, 5′-GAGAGGCATGAGGACAGGC-3′), and β-*actin* (sense, 5′-CCTCACCCTGAAGTACCCCA-3′ and antisense, 5′-TGCCAGATTTTCTCCATGTCG-3′). The cycling conditions were as follows: 95°C for 10 min followed by 45 cycles of 95°C for 15 s, 60°C for 1 min, and 95°C for 15 s. Fluorescence thresholds (C_t) were determined automatically by software, with efficiencies of amplification for the studied genes ranging between 92 and 110%. The ΔC_t value for each cDNA sample was calculated by subtracting the C_t value of the reference gene β-actin from the C_t value of the target sequence. The fold increase of mRNA expression was calculated following the manufacturer's instructions and using a standard formula, fold increase = $2^{-\Delta\Delta Ct}$.

Knockdown of *CD11b* with siRNA in THP-1 cells

Control siRNA (QIAGEN) or CD11b siRNA (4392420/siRNA ID s7566; Thermo Fisher Scientific) were transfected into THP-1 cells using an HVJ-Envelope derived from Sendai virus (GenomONE-Neo EX, COSMO BIO Co. Ltd.) according to the manufacturer's instructions. After 24-hour incubation with siRNAs, nonadherent cells were collected and transferred to a new 24-well plate where they were activated with PMA (100 ng/ml) overnight. The next day, PMA-activated transfected THP-1 cells were harvested and were assayed for CD11b expression by Western blot. In parallel, fresh complete RPMI 1640 medium was added, and the cells were activated with MDP and Tc CM for 18 hours and were assayed for *COX2* and *ILB* mRNA expressions.

Western blot analysis

Nuclear factor κB

Nuclear extracts were prepared from monocytes as previously described (*57*). Briefly, harvested and pelleted monocytes were incubated in 400 μl of cold buffer A [10 mM Hepes (pH 7.9), 10 mM KCl, 0.1 mM EDTA, 10 mM EGTA, 1 mM dithiothreitol (DTT), and protease inhibitors (PI)] on ice for 15 min followed by addition of

25 μl of 10% NP-40 followed by vortexing and centrifugation at 15,000 rpm for 1 min. The supernatant was removed, and the nuclear pellet was resuspended in ice-cold buffer C [20 mM Hepes (pH 7.9), 0.4 M NaCl, 1 mM EDTA, 1 mM EGTA, 1 mM DTT, and PI], incubated on ice with vigorous shaking for 15 min, and centrifuged at 15,000 rpm for 1 min. The supernatant was harvested, and proteins were resolved using 7.5% TGX precast gel (Bio-Rad).

CD11b

THP-1 cells were lysed in 1% NP-40 lysis buffer on ice for 30 min. Total cell lysates were resolved using 6% TGX Novex gel (Invitrogen).

GP1bα

Tc CM, M8I-treated Tc CM, or NSTc CM were concentrated 3- to 18-fold using a 50-kDa MWCO Centrifugal Filter Unit, mixed 1:1 with 2× sample buffer (Bio-Rad, catalog no. 161-0737), and boiled for 5 min. Human platelets were lysed in 1% NP-40 lysis buffer (Invitrogen) on ice for 30 min. Concentrated Tc CM, NSTc CM, M8I-treated Tc CM, platelet extracts, and mouse NS0 myeloma cell line–derived human rGPIbα protein (120 kDa; R&D systems, catalog no. 4067-GP-050) were resolved using 7.5% TGX precast gel (Bio-Rad).

After SDS-PAGE, the proteins were transferred to polyvinylidene difluoride membranes and probed with the following antibodies: rabbit anti–NF-κB p65 (1:1000; Cell Signaling Technology, catalog no. 8242 or 4764); mouse anti-αM integrin (CD11b/CD42b) (1:1000; Santa Cruz Biotechnology, catalog no. sc-515923); mouse anti–TATA-binding protein (1:2000; catalog no. ab818) and mouse HRP–anti-GAPDH (1:30,000; catalog no. ab9482) (all from Abcam); and donkey HRP–anti-rabbit and sheep HRP–anti-mouse (1:10,000; both from GE Healthcare). The GPIbα protein was detected using mouse anti-CD42b Ab clone SZ2 that recognizes the sulfated tyrosine sequence (epitope 269-282) in GPIbα (Santa Cruz Biotechnology, catalog no. sc-59052) followed by biotin anti-mouse IgG1 rabbit mAb clone RM106 (1:5000; RevMAb Biosciences, catalog no. 31-1002-02) and streptavidin-HRP (1:10,000; Abcam, catalog no. ab7403). Densitometry was performed using Gel Doc XR+ Gel Documentation System (Bio-Rad).

Staining of CD3 bead–purified T cells and of NS T cells with anti-CD41a antibodies

CD3 bead–purified T cells, NS T cells, and platelets were stained with mouse anti–CD41a-FITC mAb (clone HIP8; Thermo Fisher Scientific, catalog no. 11-0419-42) or with mouse IgG1 isotype control, washed twice, and analyzed using LSRII Flow Cytometer (BD Biosciences) and FlowJo 10.1 software (TreeStar).

Sorting of T cells and testing of PGE_2-inducing activity of sorted T cells

PBMCs were stained with the following antibodies: anti–CD41a-FITC (clone HIP8; Thermo Fisher Scientific), anti–CD4–Alexa 700 (clone OKT4; BioLegend), anti–CD8-PE.Cy5 (clone RPA-T8; BD Biosciences), anti–CD45-PE (clone REA747; Miltenyi Biotec), and with Live/Dead Fixable Aqua Dead Cell stain Kit (Thermo Fisher Scientific) at 4°C for 30 min. Labeled cells were washed twice and were sorted into $CD45^+CD41a^-CD4^+$ and $CD45^+CD41a^-CD8^+$ cell subsets using BD FACSAria Fusion Cell Sorter (BD Biosciences). The gating strategy is described in the legend to fig. S4.

Sorted $CD45^+CD41a^-CD4^+$ and $CD45^+CD41a^-CD8^+$ were stained with mouse anti–CD3-APC mAb (clone HIT3; BioLegend) and were analyzed using LSRII Flow Cytometer and FlowJo 10.1 software.

Sorted $CD45^+CD41a^-CD4^+$ and $CD45^+CD41a^-CD8^+$ cells were combined and cultured at 15×10^6/ml with CD3 microbeads at 3.0 μl/ml in RPMI 1640 medium with 1% FBS and supplements at 37°C and 5% CO_2 overnight. CM from cultured sorted T cells was collected and assayed for the induction of *COX2* mRNA and PGE_2 in monocytes.

In vivo experiments in rabbits and mice

Female NZW rabbits weighting 4 kg were purchased from Charles River Laboratories. One week before each experiment, a silastic central venous catheter was surgically implanted under general anesthesia into the right jugular vein in the ventrolateral portion of the right side of the neck. The catheter access port exited the body between the shoulder blades and was flushed daily with sterile saline to preserve patency. Animals were injected with MDP (10 or 30 μg/kg) in 1 ml of PBS or with 1 ml of PBS intramuscularly. Rectal body temperature was measured at time 0, then hourly for 8 hours, and at 24-, 48-, and 72-hour time points using a SureTemp Plus thermometer (Welch Allyn). Immediately before each temperature measurement, 4 ml of whole blood was collected via the silastic central venous catheter.

Female αM-deficient mice (B6.129S4-Itgamtm1Myd/J), CD18-deficient mice (B6.129S7-Itgb2tm1Bay/J), and age-matched WT control mice were purchased from the Jackson laboratory. Mice were injected with 1500 μg of MDP in 500 μl of PBS or with 500 μl of PBS as a control intramuscularly using a 25-gauge needle. Two hours after treatment, mice were euthanized, and spleens and livers were collected. Spleens and livers were homogenized using Precellys 24 tissue homogenizer (Bertin Instruments) following the manufacturer's instructions. Total RNA was isolated using RNeasy Plus Universal Kits per the manufacturer's protocol. cDNAs were prepared using a Reverse Transcriptase SuperScript VILO (Life Technologies). qPCR was performed using Power SYBR Green (Applied Biosystems) and a QuantStudio 6 Flex Real-Time PCR system (Applied Biosystems). The following primer pairs were used for amplification of mouse *COX-2* and β-*actin*: *Cox2* (sense, 5′-GTACAAGCAGTGGCAAAGGC-3′ and antisense, 5′-AGAAGCGTTTGCGGTACTCA-3′) and *m*β-*actin* (sense, 5′-ACTGTCGAGTCGCGTCCA-3′ and antisense, 5′-ATCCATGGCGAACTGGTGG-3′). All experimental procedures were approved by the CBER Institutional Animal Care and Use Committee.

Measurements of PGE_2 and CRP in rabbit blood

PGE_2 and CRP were detected in rabbit plasma and sera, respectively, using a PGE_2 EIA (Assay Designs) and C-Reactive Protein ELISA kits (Alpco Immunoassays) in triplicate.

Statistical analysis

Data are means ± SD. Data were analyzed with unpaired two-tailed Student's *t* test. In all tests, P values of ≤0.05 were considered statistically significant. Sample sizes for each experimental condition are provided in the figure legends.

SUPPLEMENTARY MATERIALS

stke.sciencemag.org/cgi/content/full/12/602/eaat6023/DC1

Fig. S1. PGE_2 dose response in monocytes treated with MDP alone or with MDP in the presence of Tc CM.

Fig. S2. CM from CD3 bead–treated, negatively selected T cells increased PGE_2 production in monocytes activated with MDP.

Fig. S3. Tc CM strongly augmented production of IL-8 and only minimally increased that of RANTES and IL-12 p40 in monocytes activated with MDP.

Fig. S4. Production of PGE_2 in monocytes activated with MDP and Tc CM is IL-1β independent.

Fig. S5. CM from CD3 bead–treated, negatively selected T cells increased *COX2* mRNA expression in monocytes activated with MDP.
Fig. S6. Production of IL-1β and IL-6 in monocytes activated with MDP and Tc CM is sensitive to RIP2 kinase inhibitor erlotinib.
Fig. S7. Western blot of NF-κB p65 in nuclear extracts of monocytes activated with MDP and Tc CM in the absence or presence of erlotinib.
Fig. S8. Tc CM but not NSTc CM induced calcium flux in monocytes.
Fig. S9. Flow cytometry of bead-purified T cells with antibodies to CD41a.
Fig. S10. Gating strategy to exclude presence of $CD41a^+$ platelets in subsets of sorted $CD4^+$ and $CD8^+$ T cells.
Fig. S11. CM from sort-purified T cells incubated with CD3 beads overnight induced *COX2* mRNA and PGE_2 in monocytes activated with MDP.
Fig. S12. Platelets did not induce PGE_2 in MDP-treated monocytes.
Fig. S13. *Cox2* mRNA C_t values in the spleen and liver of WT, CD18 KO, and αM KO mice injected with MDP or PBS.
Fig. S14. rGPIbα increased PGE_2, IL-1β, and IL-6 in MDP-treated monocytes.
Fig. S15. Western blot of NF-κB p65 in nuclear extracts prepared from monocytes activated with MDP and rGPIbα.
Table S1. Production of PGE_2 in monocytes activated with MDP and Tc CM but not with MDP and NSTc CM.
Table S2. Increased PGE_2-inducing activity in concentrated Tc CM.
Table S3. List of proteins increased twofold or higher in Tc CM compared with NSTc CM.
View/request a protocol for this paper from *Bio-protocol*.

REFERENCES AND NOTES

1. W. Zhou, V. Pool, J. K. Iskander, R. English-Bullard, R. Ball, R. P. Wise, P. Haber, R. P. Pless, G. Mootrey, S. S. Ellenberg, M. M. Braun, R. T. Chen, Surveillance for safety after immunization: Vaccine Adverse Event Reporting System (VAERS)—United States, 1991–2001. *MMWR Surveill. Summ.* **52**, 1–24 (2003).
2. A. I. Ivanov, A. A. Romanovsky, Prostaglandin E_2 as a mediator of fever: Synthesis and catabolism. *Front. Biosci.* **9**, 1977–1993 (2004).
3. A. A. Romanovsky, A. A. Steiner, K. Matsumura, Cells that trigger fever. *Cell Cycle* **5**, 2195–2197 (2006).
4. Z. Li, V. Perlik, C. Feleder, Y. Tang, C. M. Blatteis, Kupffer cell-generated PGE_2 triggers the febrile response of guinea pigs to intravenously injected LPS. *Am. J. Physiol. Regul. Integr. Comp. Physiol.* **290**, R1262–R1270 (2006).
5. U. C. Kopp, M. Z. Cicha, L. A. Smith, PGE_2 increases release of substance P from renal sensory nerves by activating the cAMP-PKA transduction cascade. *Am. J. Physiol. Regul. Integr. Comp. Physiol.* **282**, R1618–R1627 (2002).
6. K. Kwong, L.-Y. Lee, PGE_2 sensitizes cultured pulmonary vagal sensory neurons to chemical and electrical stimuli. *J. Appl. Physiol.* **93**, 1419–1428 (2002).
7. K. Takeuchi, S. Kato, M. Takeeda, Y. Ogawa, M. Nakashima, M. Matsumoto, Facilitation by endogenous prostaglandins of capsaicin-induced gastric protection in rodents through EP_2 and IP receptors. *J. Pharmacol. Exp. Ther.* **304**, 1055–1062 (2003).
8. A. A. Romanovsky, A. I. Ivanov, E. K. Karman, Blood-borne, albumin-bound prostaglandin E_2 may be involved in fever. *Am. J. Physiol.* **276**, R1840–R1844 (1999).
9. C. M. Blatteis, The onset of fever: New insights into its mechanism. *Prog. Brain Res.* **162**, 3–14 (2007).
10. A. Adam, R. Ciorbaru, F. Ellouz, J.-F. Petit, E. Lederer, Adjuvant activity of monomeric bacterial cell wall peptidoglycans. *Biochem. Biophys. Res. Commun.* **56**, 561–567 (1974).
11. A. G. Johnson, Molecular adjuvants and immunomodulators: New approaches to immunization. *Clin. Microbiol. Rev.* **7**, 277–289 (1994).
12. S. E. Girardin, I. G. Boneca, J. Viala, M. Chamaillard, A. Labigne, G. Thomas, D. J. Philpott, P. J. Sansonetti, Nod2 is a general sensor of peptidoglycan through muramyl dipeptide (MDP) detection. *J. Biol. Chem.* **278**, 8869–8872 (2003).
13. N. Inohara, Y. Ogura, A. Fontalba, O. Gutierrez, F. Pons, J. Crespo, K. Fukase, S. Inamura, S. Kusumoto, M. Hashimoto, S. J. Foster, A. P. Moran, J. L. Fernandez-Luna, G. Nunez, Host recognition of bacterial muramyl dipeptide mediated through NOD2. Implications for Crohn's disease. *J. Biol. Chem.* **278**, 5509–5512 (2003).
14. W. Strober, P. J. Murray, A. Kitani, T. Watanabe, Signalling pathways and molecular interactions of NOD1 and NOD2. *Nat. Rev. Immunol.* **6**, 9–20 (2006).
15. K. S. Kobayashi, M. Chamaillard, Y. Ogura, O. Henegariu, N. Inohara, G. Nunez, R. A. Flavell, Nod2-dependent regulation of innate and adaptive immunity in the intestinal tract. *Science* **307**, 731–734 (2005).
16. R. K. Gupta, G. R. Siber, Adjuvants for human vaccines—Current status, problems and future prospects. *Vaccine* **13**, 1263–1276 (1995).
17. W. Keitel, R. Couch, N. Bond, S. Adair, G. Van Nest, C. Dekker, Pilot evaluation of influenza virus vaccine (IVV) combined with adjuvant. *Vaccine* **11**, 909–913 (1993).
18. J. O. Kahn, F. Sinangil, J. Baenziger, N. Murcar, D. Wynne, R. L. Coleman, K. S. Steimer, C. L. Dekker, D. Chernoff, Clinical and immunologic responses to human immunodeficiency virus (HIV) type 1SF2 gp120 subunit vaccine combined with MF59 adjuvant with or without muramyl tripeptide dipalmitoyl phosphatidylethanolamine in non-HIV-infected human volunteers. *J Infect Dis.* **170**, 1288–1291 (1994).
19. M. C. Keefer, B. S. Graham, M. J. McElrath, T. J. Matthews, D. M. Stablein, L. Corey, P. F. Wright, D. Lawrence, P. E. Fast, K. Weinhold, R.-H. Hsieh, D. Chernoff, C. Dekker, R. Dolin, Safety and immunogenicity of Env 2-3, a human immunodeficiency virus type 1 candidate vaccine, in combination with a novel adjuvant, MTP-PE/MF59. NIAID AIDS Vaccine Evaluation Group. *AIDS Res. Hum. Retroviruses* **12**, 683–693 (1996).
20. M. C. Keefer, M. Wolff, G. J. Gorse, B. S. Graham, L. Corey, M. L. Clements-Mann, N. Verani-Ketter, S. Erb, C. M. Smith, R. B. Belshe, L. J. Wagner, M. J. McElrath, D. H. Schwartz, P. Fast, Safety profile of phase I and II preventive HIV type 1 envelope vaccination: Experience of the NIAID AIDS Vaccine Evaluation Group. *AIDS Res. Hum. Retroviruses* **13**, 1163–1177 (1997).
21. M. Zaitseva, T. Romantseva, K. Blinova, J. Beren, L. Sirota, D. Drane, H. Golding, Use of human MonoMac6 cells for development of in vitro assay predictive of adjuvant safety in vivo. *Vaccine* **30**, 4859–4865 (2012).
22. Y. Endo, K. Blinova, T. Romantseva, H. Golding, M. Zaitseva, Differences in PGE_2 production between primary human monocytes and differentiated macrophages: Role of IL-1β and TRIF/IRF3. *PLOS ONE* **9**, e98517 (2014).
23. M. Murakami, I. Kudo, Recent advances in molecular biology and physiology of the prostaglandin E_2-biosynthetic pathway. *Prog. Lipid Res.* **43**, 3–35 (2004).
24. Y. Ogura, N. Inohara, A. Benito, F. F. Chen, S. Yamaoka, G. Núñez, Nod2, a Nod1/Apaf-1 family member that is restricted to monocytes and activates NF-κB. *J. Biol. Chem.* **276**, 4812–4818 (2001).
25. J.-H. Park, Y.-G. Kim, C. McDonald, T.-D. Kanneganti, M. Hasegawa, M. Body-Malapel, N. Inohara, G. Núñez, RICK/RIP2 mediates innate immune responses induced through Nod1 and Nod2 but not TLRs. *J. Immunol.* **178**, 2380–2386 (2007).
26. T. Tanabe, N. Tohnai, Cyclooxygenase isozymes and their gene structures and expression. *Prostaglandins Other Lipid Mediat.* **68-69**, 95–114 (2002).
27. J.-H. Wong, K.-H. Ho, S. Nam, W.-L. Hsu, C.-H. Lin, C.-M. Chang, J.-Y. Wang, W.-C. Chang, Store-operated Ca^{2+} entry facilitates the lipopolysaccharide-induced cyclooxygenase-2 expression in gastric cancer cells. *Sci. Rep.* **7**, 12813 (2017).
28. T. Murakami, J. Ockinger, J. Yu, V. Byles, A. McColl, A. M. Hofer, T. Horng, Critical role for calcium mobilization in activation of the NLRP3 inflammasome. *Proc. Natl. Acad. Sci. U.S.A.* **109**, 11282–11287 (2012).
29. E. E. Gardiner, D. Karunakaran, Y. Shen, J. F. Arthur, R. K. Andrews, M. C. Berndt, Controlled shedding of platelet glycoprotein (GP)VI and GPIb-IX-V by ADAM family metalloproteinases. *J. Thromb. Haemost.* **5**, 1530–1537 (2007).
30. Y. Shen, G. M. Romo, J.-f. Dong, A. Schade, L. V. McIntire, D. Kenny, J. C. Whisstock, M. C. Berndt, J. A. Lopez, R. K. Andrews, Requirement of leucine-rich repeats of glycoprotein (GP) Ibα for shear-dependent and static binding of von Willebrand factor to the platelet membrane GP Ib-IX-V complex. *Blood* **95**, 903–910 (2000).
31. H. Ebsen, A. Schröder, D. Kabelitz, O. Janssen, Differential surface expression of ADAM10 and ADAM17 on human T lymphocytes and tumor cells. *PLOS ONE* **8**, e76853 (2013).
32. Q. Feng, N. Shabrani, J. N. Thon, H. Huo, A. Thiel, K. R. Machlus, K. Kim, J. Brooks, F. Li, C. Luo, E. A. Kimbrel, J. Wang, K.-S. Kim, J. Italiano, J. Cho, S.-J. Lu, R. Lanza, Scalable generation of universal platelets from human induced pluripotent stem cells. *Stem Cell Rep.* **3**, 817–831 (2014).
33. D. I. Simon, Z. Chen, H. Xu, C. Q. Li, J.-f. Dong, L. V. McIntire, C. M. Ballantyne, L. Zhang, M. I. Furman, M. C. Berndt, J. A. López, Platelet glycoprotein ibα is a counterreceptor for the leukocyte integrin Mac-1 (CD11b/CD18). *J. Exp. Med.* **192**, 193–204 (2000).
34. J. Ng-Sikorski, R. Andersson, M. Patarroyo, T. Andersson, Calcium signaling capacity of the CD11b/CD18 integrin on human neutrophils. *Exp. Cell Res.* **195**, 504–508 (1991).
35. D. C. Altieri, S. J. Stamnes, C. G. Gahmberg, Regulated Ca^{2+} signalling through leukocyte CD11b/CD18 integrin. *Biochem. J.* **288**, 465–473 (1992).
36. T. P. Ugarova, D. A. Solovjov, L. Zhang, D. I. Loukinov, V. C. Yee, L. V. Medved, E. F. Plow, Identification of a novel recognition sequence for integrin $\alpha_M \beta_2$ within the γ-chain of fibrinogen. *J. Biol. Chem.* **273**, 22519–22527 (1998).
37. M. Nakanishi, D. W. Rosenberg, Multifaceted roles of PGE_2 in inflammation and cancer. *Semin. Immunopathol.* **35**, 123–137 (2013).
38. K. Kobayashi, N. Inohara, L. D. Hernandez, J. E. Galán, G. Núñez, C. A. Janeway, R. Medzhitov, R. A. Flavell, RICK/Rip2/CARDIAK mediates signalling for receptors of the innate and adaptive immune systems. *Nature* **416**, 194–199 (2002).
39. J.-K. Lee, S.-H. Kim, E. C. Lewis, T. Azam, L. L. Reznikov, C. A. Dinarello, Differences in signaling pathways by IL-1β and IL-18. *Proc. Natl. Acad. Sci. U.S.A.* **101**, 8815–8820 (2004).
40. S. E. Plevy, J. H. Gemberling, S. Hsu, A. J. Dorner, S. T. Smale, Multiple control elements mediate activation of the murine and human interleukin 12 p40 promoters: Evidence of functional synergy between C/EBP and Rel proteins. *Mol. Cell. Biol.* **17**, 4572–4588 (1997).

41. P. Génin, M. Algarté, P. Roof, R. Lin, J. Hiscott, Regulation of RANTES chemokine gene expression requires cooperativity between NF-κB and IFN-regulatory factor transcription factors. *J. Immunol.* **164**, 5352–5361 (2000).
42. N. Mason, J. Aliberti, J. C. Caamano, H.-C. Liou, C. A. Hunter, Cutting edge: Identification of c-Rel-dependent and -independent pathways of IL-12 production during infectious and inflammatory stimuli. *J. Immunol.* **168**, 2590–2594 (2002).
43. J. Liu, X. Ma, Interferon regulatory factor 8 regulates RANTES gene transcription in cooperation with interferon regulatory factor-1, NF-κB, and PU.1. *J. Biol. Chem.* **281**, 19188–19195 (2006).
44. K. J. Clemetson, J. M. Clemetson, Platelet GPIb complex as a target for anti-thrombotic drug development. *Thromb. Haemost.* **99**, 473–479 (2008).
45. A. T. Nurden, K. Freson, U. Seligsohn, Inherited platelet disorders. *Haemophilia* **18**, 154–160 (2012).
46. E. I. Peerschke, Platelet membrane glycoproteins. *Functional characterization and clinical applications*. *Am. J. Clin. Pathol.* **98**, 455–463 (1992).
47. K. J. Clemetson, H. Y. Naim, E. F. Luscher, Relationship between glycocalicin and glycoprotein Ib of human platelets. *Proc. Natl. Acad. Sci. U.S.A.* **78**, 2712–2716 (1981).
48. G. M. Romo, J.-F. Dong, A. J. Schade, E. E. Gardiner, G. S. Kansas, C. Q. Li, L. V. McIntire, M. C. Berndt, J. A. López, The glycoprotein Ib-IX-V complex is a platelet counterreceptor for P-selectin. *J. Exp. Med.* **190**, 803–814 (1999).
49. J. E. B. Fox, L. P. Aggerbeck, M. C. Berndt, Structure of the glycoprotein Ib.IX complex from platelet membranes. *J. Biol. Chem.* **263**, 4882–4890 (1988).
50. M. A. Arnaout, Structure and function of the leukocyte adhesion molecules CD11/CD18. *Blood* **75**, 1037–1050 (1990).
51. C. A. Dinarello, R. J. Elin, L. Chedid, S. M. Wolff, The pyrogenicity of the synthetic adjuvant muramyl dipeptide and two structural analogues. *J Infect Dis.* **138**, 760–767 (1978).
52. L. A. Chedid, M. A. Parant, F. M. Audibert, G. J. Riveau, F. J. Parant, E. Lederer, J. P. Choay, P. L. Lefrancier, Biological activity of a new synthetic muramyl peptide adjuvant devoid of pyrogenicity. *Infect. Immun.* **35**, 417–424 (1982).
53. E. A. Clark, J. S. Brugge, Integrins and signal transduction pathways: The road taken. *Science* **268**, 233–239 (1995).
54. C. G. Figdor, W. S. Bont, I. Touw, J. de Roos, E. E. Roosnek, J. E. de Vries, Isolation of functionally different human monocytes by counterflow centrifugation elutriation. *Blood* **60**, 46–53 (1982).
55. D. Kryndushkin, W. W. Wu, R. Venna, M. A. Norcross, R. F. Shen, V. A. Rao, Complex nature of protein carbonylation specificity after metal-catalyzed oxidation. *Pharm. Res.* **34**, 765–779 (2017).
56. W. W. Wu, G. Wang, P. A. Insel, C.-T. Hsiao, S. Zou, B. Martin, S. Maudsley, R.-F. Shen, Discovery- and target-based protein quantification using iTRAQ and pulsed Q collision induced dissociation (PQD). *J. Proteomics* **75**, 2480–2487 (2012).
57. E. Schreiber, P. Matthias, M. M. Müller, W. Schaffner, Rapid detection of octamer binding proteins with 'mini-extracts', prepared from a small number of cells. *Nucleic Acids Res.* **17**, 6419 (1989).

Acknowledgments: We thank B. Golding and S. Khurana for comments on the manuscript and valuable discussions. **Funding:** This work was supported by the Intramural Research Program of CBER, FDA. **Author contributions:** F.L. and Y.E. designed and performed experiments. T.R. and A.A. provided technical help. W.W.W. and R.-F.S. performed MS and data analysis. H.G. contributed to project design. M.Z. conceived the idea and designed the experimental plan. F.L., Y.E., H.G., and M.Z. discussed the results and wrote the manuscript. **Competing interests:** The authors declare that they have no competing interests. **Data and materials availability:** All data needed to evaluate the conclusions in the paper are present in the paper or the Supplementary Materials.

Submitted 16 March 2018
Resubmitted 10 April 2019
Accepted 3 September 2019
Published 8 October 2019
10.1126/scisignal.aat6023

Citation: F. Liu, Y. Endo, T. Romantseva, W. W. Wu, A. Akue, R.-F. Shen, H. Golding, M. Zaitseva, T cell–derived soluble glycoprotein GPIbα mediates PGE_2 production in human monocytes activated with the vaccine adjuvant MDP. *Sci. Signal.* **12**, eaat6023 (2019).

Science Signaling

T cell–derived soluble glycoprotein GPIbα mediates PGE_2 production in human monocytes activated with the vaccine adjuvant MDP

Fengjie Liu, Yukinori Endo, Tatiana Romantseva, Wells W. Wu, Adovi Akue, Rong-Fong Shen, Hana Golding and Marina Zaitseva

Sci. Signal. **12** (602), eaat6023.
DOI: 10.1126/scisignal.aat6023

Vaccine reactions are a multicellular affair

Vaccine adjuvants can cause adverse, sometimes life-threatening, immune reactions in patients. The adjuvant MDP activates monocytes to release an inflammatory prostaglandin and cytokines. However, Liu *et al.* found that MDP administration to human monocytes alone was insufficient to produce the prostaglandin response that they saw when it was administered to rabbits. Instead, the authors found that MDP induced T cells to release the glycoprotein GPIbα (better known in platelets), which stimulated Ca^{2+} signaling by a receptor on the monocytes, resulting in prostaglandin production. Knocking out the GPIb α receptor prevented the inflammatory response to MDP in mice. This multicellular mechanism may underlie adverse vaccine reactions in humans.

Science Signaling (ISSN 1937-9145) is published by the American Association for the Advancement of Science, 1200 New York Avenue NW, Washington, DC 20005. The title *Science Signaling* is a registered trademark of AAAS.